91602
new 82-10

LEGAL NOTICE

This report was prepared by Ontario Hydro and, while effort has been made to assure the accuracy and applicability of the material contained herein, neither Ontario Hydro nor any person acting on its behalf:

(a) makes any warranty, express or implied with respect to the use of any information, apparatus, method or process disclosed in this report or that such use does not infringe on or interfere with privately owned rights; or

(b) assumes any liability with respect to the use of, or for damages resulting from the use of, any information, apparatus, method or process disclosed in this report.

COMPLIMENTARY COPY
Please Credit Ontario Hydro Research if Reproduced in Whole or in Part

ontario hydro
research division

H3DTAP VERSION 1 - A THREE DIMENSIONAL FINITE ELEMENT PROGRAM FOR THERMAL AND MOLECULAR DIFFUSION ANALYSIS

Report No. 91-102-K

D.R. Metzger
Engineer
Applied Mechanics Section
Mechanical Research Department

ABSTRACT

The finite element code H3DTAP Version 1 is a general three dimensional heat transfer and diffusion analysis package that has been developed at Ontario Hydro. The main need for such a code is that commercially available numerical analysis software does not address many of the corporation's highly specialized problems involving nonlinear heat transfer and molecular diffusion. This report outlines the analytical capabilities of H3DTAP, and presents the pertinent theory underlying the numerical methods used in the program. Also, a users manual is included describing the format of the input data required in the program.

H3DTAP includes one, two, and three dimensional continuum elements in addition to axisymmetric versions of the one and two dimensional elements. These elements can be used to model very general diffusion problems ranging from linear steady state to nonlinear transient situations. The capability to do coupled nonlinear thermal/molecular diffusion analysis has also been established by making effective use of new explicit transient analysis methods.

Modifications and additions to the program are accomodated by its modular structure. Thus, H3DTAP can be adapted to solve new and more complex problems by adding to the existing base of subroutines rather than developing specialized programs from the ground up.

job	file	date	report no.
21-524-051	825.2	July 12, 1991	91-102-K

91602
new 82-10

92-03489/

ontario hydro
research division

EXECUTIVE SUMMARY

H3DTAP VERSION 1 - A THREE DIMENSIONAL FINITE ELEMENT PROGRAM FOR THERMAL AND MOLECULAR DIFFUSION ANALYSIS

D.R. Metzger
Applied Mechanics Section
Mechanical Research Department

The finite element code H3DTAP Version 1 is a general three dimensional heat transfer and diffusion analysis package that has been developed at Ontario Hydro. H3DTAP is an acronym for Hydro 3 Dimensional Thermal Analysis Program. The main need for such a code is that commercially available numerical analysis software does not address many of the corporation's highly specialized problems involving nonlinear heat transfer and molecular diffusion. For example, the ability to do three dimensional analysis of the hydride blister growth encountered in CANDU fuel channels does not exist in commercial software. This report outlines the analytical capabilities of H3DTAP, and presents the pertinent theory underlying the numerical methods used in the program. Also, a users manual, included as an appendix, describes the format of the input data required in the program.

H3DTAP includes one, two, and three dimensional continuum elements in addition to axisymmetric versions of the one and two dimensional elements. These elements can be used to model very general diffusion problems ranging from linear steady state to nonlinear transient situations. Also, the capability to do coupled nonlinear thermal/molecular diffusion analysis has been established by making effective use of new explicit transient analysis methods. With state of the art methods, finite element models involving tens of thousands of elements can be run, even on modest engineering workstations.

Written in FORTRAN 77, H3DTAP presently runs on DEC computers using either VMS or UNIX operating systems. Transfer to other computing environments is possible with minimal effort. Modifications and additions, to accomodate new problems, are straightforward because of the modular structure used throughout the program. Thus, H3DTAP can be adapted to solve new and more complex problems by adding to the existing base of subroutines rather than developing specialized programs from the ground up. This is a very important aspect of such a program since many new specialized applications are anticipated in the future.

job	file	date	report no
21-524-051	825.2	July 12, 1991	91-102-K

TABLE OF CONTENTS

Page

ABSTRACT
EXECUTIVE SUMMARY
LIST OF FIGURES iii

1.0 INTRODUCTION 1

2.0 PROGRAM STRUCTURE 2

3.0 THEORETICAL BACKGROUND 3
- 3.1 Heat Transfer 3
  - 3.1.1 General Equations 3
  - 3.1.2 Linear Analysis 4
  - 3.1.3 Nonlinear Analysis 4
  - 3.1.4 Network Analogue for Explicit Time Integration 7
- 3.2 Hydrogen Diffusion Analysis 8
  - 3.2.1 Governing Equations 8
  - 3.2.2 Precipitation and Dissolution Modelling 10
  - 3.2.3 Nonlinear Coupled Thermal/Hydrogen Diffusion Analysis 12

4.0 ELEMENT REPRESENTATION 15
- 4.1 Isoparametric Continuum Elements 15
  - 4.1.1 1-D Continuum Element 15
  - 4.1.2 2-D Continuum Element 16
  - 4.1.3 3-D Continuum Elements 16
  - 4.1.4 Boundary Conditions 17
- 4.2 Contact Elements 18
  - 4.2.1 General Derivation 18
  - 4.2.2 1-D Contact Element 20
  - 4.2.3 2-D Contact Element 20
  - 4.2.4 3-D Contact Element 21
  - 4.2.5 Gap Dependent Contacts 21

5.0 CONCLUDING REMARKS 21

ACKNOWLEDGMENTS 23

REFERENCES 24

APPENDIX A A-1

APPENDIX B B-1

DISTRIBUTION ..... last

LIST OF FIGURES

2.1 Tree Structure of Main Program
2.2 Tree Structure of Analysis Modules

3.1.1 Network Representation of Continuum Element

3.2.1 Temperature Dependence of Terminal Solid Solubility
3.2.2 Modelling Effect of Precipitation on Element Properties
3.2.3 Flowchart of Coupled Thermal/Hydrogen Diffusion Analysis

4.1.1 Continuum Element Node Numbering Order
4.1.2 Boundary Conditions

4.2.1 Convection From a Surface
4.2.2 Contact Element Node Numbering Order
4.2.3 Conduction Through Variable Thickness Gap

5.1 Mesh for Pickering Unit 2 with Multiple Contacts Between Pressure Tube and Calandria Tube
5.2 Temperature Distribution in P2 G16 for One 2.5 mm Radius Contact

ontario hydro
research division

To Dr. D. Mills
Director of Research

H3DTAP VERSION 1 - A THREE DIMENSIONAL FINITE ELEMENT PROGRAM FOR THERMAL AND MOLECULAR DIFFUSION ANALYSIS

1.0 INTRODUCTION

The need for an in-house analysis program stems from the highly specialized problems involving diffusion processes encountered at Ontario Hydro. For example, the capability to model hydrogen diffusion and subsequent hydride formation found in CANDU fuel channels is not available in commercial analysis software which is intended for more generic problems. Even when commercial software has the necessary capabilities, performance limitations of such programs can result in significant restrictions on the level of detail that can be modelled.

This report describes the in-house finite element program H3DTAP (**H**ydro **3**-**D**imensional **T**hermal **A**nalysis **P**rogram) Version 1.0 which is applicable to a variety of field problems. In particular, problems involving:

1) steady state heat transfer
2) transient heat transfer (linear and nonlinear)
3) hydrogen diffusion
4) coupled heat transfer/hydrogen diffusion

can be modelled in one, two, or three dimensions. Axisymmetric problems in one and two dimensions can also be modelled.

The actual computer code is based on the program H3DMAP [1] used for analysis of structures. H3DTAP retains as much of the input data format of H3DMAP as possible to enable concurrent thermal and structural analysis using the same basic input data. However, diffusion problems require significantly different material properties and such input data for H3DTAP is necessarily different from H3DMAP.

One major difference between structural and thermal analysis is the convective heat transfer boundary condition in thermal problems. There is also the possibility of the connection of two conducting bodies via a thermal contact. In addition to these situations is the effect of radiative heat transfer either between a body and ambient space or between two conducting bodies. H3DTAP uses a novel contact element concept to treat the convection, contact, and radiation boundary conditions. This approach provides a high degree of flexibility in the capabilities of the program with the addition of only one type of element.

Another unique feature of H3DTAP is the nonlinear transient analysis option which incorporates a very efficient formulation of explicit time integration. The inherent simplicity of explicit methods enables the treatment of very large scale problems with highly nonlinear behaviour.

The work descibed herein has been developed to provide a flexible, up-to-date analytical capability for solving increasingly sophisticated models. This report includes a description of the theory underlying all aspects of diffusion analysis encompassed by the program as well as a description of the implementation of the theory in the computer code.

2.0 PROGRAM STRUCTURE

A modular format is maintained throughout H3DTAP to simplify the process of making changes and additions to the program. The subroutines can be grouped into two main categories:

- initialization routines that read and/or process input data
- analysis modules that perform specific types of analyses.

Figure 2.1 is a tree diagram of the subroutine structure showing all initialization routines and the analysis modules. Each analysis module has its own subroutine substructure shown in figures 2.2a to 2.2e. All coding is done in FORTRAN-77 and H3DTAP is compiled for execution on VAX/VMS and UNIX computing facilities. Dynamic storage allocation is used to minimize computer core memory requirements during execution. The numerous files used by the program during execution are listed in Table 1.

Table 1

H3DTAP File Usage

Unit Number	*File Name*	*Description*
1	*.H3DTAP_INPUT	input data
2	*.H3DTAP_ELEM	element definition output
3	*.H3DTAP_STIF	stiffness matrix output
4	*.H3DTAP_PLOTHIST	temperature time history output
8	*.H3DTAP_PLOTHYDR	concentration history output
12	*.H3DTAP_PLOTSTRU	temperature distribution output
13	*.H3DTAP_HYDRSTRU	concentration distribution output
15	*.H3DTAP_STATE	state dump output (not used)
16	*.H3DTAP_OUTPUT	ASCII output data
17	*.H3DTAP_LINKS	temporary link stiffness
20	*.H3DTAP_RESTART	restart file (not used)

A users manual describing the contents of the input data file is given in Appendix A.

Two post processing programs, POST_TAP and PLOT_TAP use some of these files to generate:

- coordinate and element files for plotting geometry
- nodal results files for plotting temperature or concentration distributions
- chronological results files for plotting time histories of nodal values.

A translating program, TAP2PAT, converts results files to a neutral format compatible with the commercial colour graphics program PATRAN.

3.0 THEORETICAL BACKGROUND

3.1 Heat Transfer

3.1.1 *General Equations*

The heat equation solved by H3DTAP is simply stated as

$$\vec{\nabla} \cdot [\vec{k}] \cdot \vec{\nabla} T + Q = \rho c \dot{T} \tag{3.1.1}$$

where

$\vec{\nabla}$ = the gradient operator

$[\vec{k}]$ = a tensor of thermal conductivity ($[\vec{k}]$ is assumed to be diagonal)

T = temperature

Q = internal heat generation

ρ = mass density

c = specific heat

The boundary conditions applicable to the heat equation are

$T_s = T(\vec{x},t)$ (imposed temperature) (3.1.2)

$\vec{q} \cdot \vec{n} = -q_s$ (imposed source) (3.1.3)

$\vec{q} \cdot \vec{n} = h(T_s - T_{amb})$ (convection) (3.1.4)

$\vec{q} \cdot \vec{n} = \sigma e \left(T^4 - T^4_{amb}\right)$ (radiation) (3.1.5)

The convection and radiation boundary conditions are treated by utilizing a fictitious material that characterizes convective or radiative heat transfer. In this way, only temperatures and imposed

sources (distributed or concentrated) need to be specified as boundary conditions. The theoretical basis for the convection and radiation treatment is given in a subsequent section of this report.

The application of the finite element method to the heat equation, (3.1.1), yields the system of equations

$$[K]\{T\} + [M]\{\dot{T}\} = R \tag{3.1.6}$$

Here [K] is an assembled matrix of the elemental stiffness matrices including the usual stiffness representing conductivity as well as the stiffnesses for the special convection and radiation elements. {T} is a vector of nodal temperatures, [M] is a matrix of thermal capacitance, and {R} is a vector of nodal heat source resulting from internal heat generation or imposed heat source boundary conditions. Details on the formulation of the stiffness, capacitance and load matrices are given in section 4.0 below.

3.1.2 *Linear Analysis*

The general equation can be simplified when material properties are assumed to be constant with respect to time and temperature. In this case the following assumptions are made:

1) $[\vec{k}]$, q, c, and h are constant with respect to time and temperature;

2) no radiation heat transfer is present.

In such a case, the assembled stiffness and capacitance matrices are constant.

If the problem is further assumed to be in steady state, then the finite element equations reduce to the linear algebraic system,

$$[K]\{T\} = \{R\} \tag{3.1.7}$$

which is solved by the LU decomposition method described in section 5 of [1].

If however, the problem is transient, then equation 3.1.2 must be integrated with respect to time. In H3DTAP, the implicit θ method is used where

$$\left[\frac{1}{\Delta t}[M]+\theta[K]\right]\{T\}^{t+\Delta t} + \left[\frac{-1}{\Delta t}[M]+(1-\theta)[K]\right]\{T\}^{t} = \theta\{R\}^{t+\Delta t} + (1-\theta)\{R\}^{t} \tag{3.1.8}$$

must be solved for {T} at each time step and θ is given a value between 0 and 1. This method is the usual approach used for linear transient problems and is described in more detail in [3].

3.1.3 *Nonlinear Analysis*

In general, when material properties vary with temperature and time, a nonlinear transient problem is encountered. Although the implicit θ method can be used for such problems, the need to

reconstruct and decompose the stiffness at each time step is usually impractical. Alternative methods are available with various pros and cons depending on the type of nonlinearities present. In H3DTAP, only one method, the explicit method, is used because:

1) appropriate implementation of explicit time integration is competitive with other methods in terms of CPU requirements;

2) explicit methods are simple to code and are easily maintained through upgrades to the program;

3) there is virtually no restriction on the type of nonlinearity that can be handled. This eliminates the need to have different algorithms for different types of problems.

The importance of efficient implementation of the explicit method cannot be overstressed since the conditional stability condition often requires very small time steps. Thus, the number of operations required for each time step must be kept to a minimum. In an effort to minimize operations, a few assumptions are made which introduce some approximation to the finite element equations in addition to the usual discretization and truncation errors. These assumptions are:

1) material properties are assumed to be constant within an element and are based on the average nodal values of the element;

2) the conductivity tensor is assumed to have the form

$$[\vec{k}] = k(T)\begin{bmatrix} a_x & 0 & 0 \\ 0 & a_y & 0 \\ 0 & 0 & a_z \end{bmatrix} \tag{3.1.9}$$

where a_x, a_y and a_z are constants. This allows the variation of elemental stiffness to be scaled and there is no need to reconstruct elemental stiffness;

3) Lumped capacitance is used and these values are made to depend on the corresponding nodal temperatures.

The explicit method is a special case of the Θ implicit method with $\Theta = 0$. Then equation (3.1.8) simplifies to

$$\frac{1}{\Delta t}[M]\{T\}^{t+\Delta t} - \left[\frac{1}{\Delta t}[M] - [K]\right]\{T\}^t = \{R\}^t \tag{3.1.10}$$

which can be rewritten as

$$\{T\}^{t+\Delta t} = \{T\}^t + \Delta t\,[M]^{-1}\left\{\{R\}^t - [K]\{T\}^t\right\} \tag{3.1.11}$$

The majority of the computational effort lies in computing the product

$$\{A\}' = [K]\ \{T\}' \tag{3.1.12}$$

where {A}' is simply an intermediate result. The procedure for evaluating equation (3.1.11) requires that for each element, the elemental stiffness is given by

$$[K_e] = k(T_e)\ [\bar{K}_e] \tag{3.1.13}$$

where $[\bar{K}_e]$ is a constant matrix that is computed once and stored in memory, and $k(T_e)$ is a scale factor dependent on the average temperature of the element. Then equation (3.1.12) can be evaluated for each element using the constant elemental stiffness to give

$$\{\bar{A}_e\}' = [\bar{K}_e]\ \{T_e\}' \tag{3.1.14}$$

which is then scaled to yield

$$\{A_e\}' = k(T_e)\ \{\bar{A}_e\}' \tag{3.1.15}$$

The elemental $\{A_e\}$'s are then assembled into the global {A} vector for use in equation (3.1.11). The above procedure avoids the need to scale the entire elemental stiffness matrix by scaling the $\{A_e\}$ vector instead. The total number of operations required to form {A} is

$$\#\ op. = NE*(NDOF^2 + NDOF) \tag{3.1.16}$$

where NE is the number of elements and NDOF is the number of degrees of freedom in each element. This permits very accurate estimates of the CPU time required to perform the analysis since solution time depends only on the number of elements and the number of time steps used. Furthermore, the storage required for the stiffness matrices is

$$storage = NE*(NDOF^2 - NDOF)/2 \tag{3.1.17}$$

which is directly proportional to the number of elements. This storage requirement is quite minimal when compared to the storage required for an assembled banded matrix, particularly for very large complex models. Since a global stiffness matrix is not assembled, there is no need to number nodes or elements to minimize bandwidth or frontwidth. Node and element numbering has no effect on the CPU and storage requirements. Because of the efficiency of implementation, the explicit method is of practical use in solving nonlinear steady state problems simply by running a transient solution to steady state conditions. Dynamic relaxation techniques can provide further improvement to this approach.

3.1.4 *Network Analogue for Explicit Time Integration*

The above approach of multiplying elemental stiffness with the elemental temperature vector prior to assembly can be improved upon with a simple modification. For isoparametric elements used

in a self-adjoint problem, the elemental stiffness matrix can be represented by the assemblage of many one-dimensional elements (links) connecting all possible combinations of pairs of nodes. Figure 3.1.1 shows a four noded continuum element along with its network counterpart. The 4x4 elemental stiffness matrix obtained using full quadrature can also be obtained by assembling the six 2x2 stiffness matrices for each 1-D link element. In practice, the link stiffnesses are actually determined as the off-diagonal terms of the standard continuum element stiffness. In this way, any model utilizing 1-D, 2-D, or 3-D elements can be viewed as if it were made up of a larger number of 1-D elements. There is no approximation involved in this process, and assembly of all links leads to the same global stiffness as obtained the usual way.

The advantage of considering only 1-D elements is that the matrix product, $[K_e]\{T_e\}$, can be formed and the result assembled with only one multiplication and three additions per 1-D element. Although there are many more 1-D links than 2-D or 3-D elements, the low operation count to process each link typically results in factor of four times less operations to do each explicit time step when compared to the method of multiplying the complete elemental stiffness matrix with its corresponding vector. A more comprehensive discussion about the network analogue method is given in [4].

3.2 Hydrogen Diffusion Analysis

3.2.1 *Governing Equations*

The governing differential equation for diffusion of hydrogen atoms in solid solution with metals in a temperature field is given in [5] as

$$\vec{\nabla} \cdot v_s [\vec{D}] \cdot \left\{ \vec{\nabla} c_s + \frac{c_s Q^*}{RT^2} \vec{\nabla} T \right\} + q = \dot{c} \qquad (3.2.1)$$

where

- c = concentration
- c_s = concentration in solution
- v_s = volume fraction of parent material
- Q^* = heat of transport
- R = gas constant
- T = absolute temperature
- $[\vec{D}]$ = tensor of diffusion coefficients
- $\vec{\nabla}$ = gradient operator
- q = source term representing pickup of hydrogen

Equation (3.2.1) has the same form as the convective-diffusion equation but the special form of the convective term (ie. the term involving temperature gradient) admits a transformation to make equation (3.2.1) self adjoint. The substitution

$$s = c \cdot e^{-Q^*/RT} \tag{3.2.2}$$

first noted in [6] results in a simplification of equation (3.2.1) to

$$\vec{\nabla} \cdot [\vec{D}^*] \cdot \vec{\nabla} s_s + q = e^{Q^*/RT} \dot{s} \tag{3.2.3}$$

where

$$[\vec{D}^*] = \nu_s e^{Q^*/RT} [\vec{D}] \tag{3.2.4}$$

Since the temperature field is assumed to be known through some preceeding analysis, $[\vec{D}^*]$ and exp(Q*/RT) are simply spatially dependent quantities, and equation (3.2.3) is almost of the same form as the heat equation (3.1.1). Thus, upon transforming the appropriate variables, the hydrogen diffusion can be treated with the same finite element formulation used for thermal analysis. The finite element representation of equation (3.2.3) is

$$[K]\{s_s\} + [M]\{\dot{s}\} = \{R\} \tag{3.2.5}$$

One complication in two phase molecular diffusion is caused by the presence of two dependent variables in the governing equation, (ie. s and s_s). Actually, these two quantities are not independent so that s_s can be specified knowing the history of s and temperature. Thus, in principal, there is a diagonal matrix [F] such that

$$\{s_s\} = [F]\{s\} \tag{3.2.6}$$

where the entries of [F] are path dependent functions of the total concentration and the temperature histories. With this relationship, equation (3.2.5) stated in terms of only one dependent variable becomes

$$[K][F]\{s\} + [M]\{\dot{s}\} = \{R\} \tag{3.2.7}$$

which is now nonlinear because of the dependence of [F] on the concentration history. There is also nonlinearity present due to the dependence of ν_s, and hence the effective diffusivity, on concentration. In principal, this equation could be integrated by the θ method described in [3] where

$$t^{n+1} = t^n + \Delta t \tag{3.2.8}$$

$$t^{\theta} = t^{n} + \theta\Delta t \tag{3.2.9}$$

$$\{s\}^{\theta} = (1-\theta)\{s\}^{n} + \theta\{s\}^{n+1} \tag{3.2.10}$$

$$\{\dot{s}\}^{\theta} = \frac{\{s\}^{n+1} - \{s\}^{n}}{\Delta t} \tag{3.2.11}$$

When matrices [K], [F], [M], and {R} are evaluated using properties at time t^{θ}, the implicit θ method yields

$$\left[\frac{1}{\Delta t}[M] + \theta[K][F]\right]\{s\}^{n+1} + \left[\frac{-1}{\Delta t}[M] + (1-\theta)[K][F]\right]\{s\}^{n} = (1-\theta)\{R\}^{n} + \theta\{R\}^{n+1} \tag{3.2.12}$$

Unfortunately, the nonlinear path-dependent nature of [F] is very awkward to handle and the iterative solution of the resulting set of equations is likely to be expensive in terms of CPU costs. A vast simplification results if the fully explicit method ($\theta = 0$) is used. Now, the $[F]\{s\}^{n}$ term can be replaced by $\{s_s\}^{n}$ which must be known at the beginning of the time step. The recursion equation (3.2.12) is then written as

$$\{s\}^{n+1} = \{s\}^{n} - \Delta t[M]^{-1}\left\{[K]\{s_s\}^{n} + \{R\}^{n}\right\} \tag{3.2.13}$$

Upon finding the new $\{s\}^{n+1}$, the new $\{s_s\}^{n+1}$ is determined from the mathematical model of precipitation and dissolution. Thereafter, the stiffness and source matrices are updated and the process is repeated for the next time step.

3.2.2 *Precipitation and Dissolution Modelling*

In the previous section, the finite element equations involve a nonlinear path-dependent relationship between s and s_s which must be specified in order to complete the model. Equation (3.2.13) defines the total concentration at the end of a time step by adding a change in concentration to the concentration at the beginning of the time step. This change in concentration may also change the concentration in solution subject to constraints of solubility limits of the parent material.

Figure 3.2.1 shows the temperature dependence of terminal solid solubility (TSS) for both the dissolution and precipitation processes. Further explanation behind this TSS model is given in [5] and [6]. Here, the procedure for using the TSS diagram to constrain s_s is outlined briefly.

1) find the new total concentration, $s^{n+1} = s^{n} + \Delta s^{n}$

2) find the apparent change in s_s that would result from the computed change in total concentration;

$$\Delta s_s^{n} = \Delta s^{n} / v_s^{n}$$

assuming v_s^n is constant over the time step. If $v_s = 0$, then set $\Delta s_s^n = 0$.

3) compute new apparent concentration in solution

$$\bar{s}_s^{n+1} = s_s^n + \Delta s_s^n$$

4) check new apparent concentration in solution against TSS diagram and adjust if necessary to obtain the actual new concentration in solution.

Provision must be allowed in step 2 for the dissolution of a solid blister. Also, step 4 requires additional explanation since several different cases can occur. These cases, with concentrations and TSS values normalized according to equation (3.2.2), are:

i) if $\bar{s}_s^{n+1} > TSSP$ then $s_s^{n+1} = TSSP$

ii) if $\bar{s}_s^{n+1} < TSSD$ then $s_s^{n+1} = min\{s^{n+1}, TSSD\}$

iii) otherwise $s_s^{n+1} = \bar{s}_s^{n+1}$

In Case (i) any increase in concentration cannot be maintained in solution and therefore increases the amount of precipitate. Case (ii) occurs when concentration is decreasing and apparent concentration in solution is less than or equal to TSSD. If total concentration is greater than TSSD, then existing precipitate dissolves while s_s is fixed to TSSD. When total concentration becomes less than TSSD (all hydride has dissolved) then only one phase is present and $s_s = s$. Case (iii) represents the situation where the change in s_s does not result in the crossing of either the TSSD or TSSP line during the time step so neither dissolution nor precipitation occurs.

In addition to the complications in specifying the concentration in solution, there are further details in modelling the effect of buildup of precipitate. As more and more hydride builds up, diffusion is inhibited and eventually choked off, since diffusion in the hydride phase is neglected. When the total concentration reaches the concentration of solid hydride, (c_b = 16000 ppm), no diffusion can occur since the volume fraction of the parent material available for diffusion, given by

$$v_s = \frac{c_b - c}{c_b - c_s}, \qquad (3.2.14)$$

is zero when $c = c_b$.

In the finite element model, the volume fraction of parent material varies linearly over an element as dictated by the linear shape functions and nodal volume fraction. Since diffusion is assumed to only occur in the parent material, the buildup of precipitate blocks the movement of hydrogen atoms. Physically, when v_s becomes zero at a node, additional hydrogen cannot go to that node since it is already solid hydride and diffusion is choked off. However, the volume fraction distribution in the element, when integrated over the volume of the element, will generally result

in nonzero stiffness terms that do allow more hydrogen to travel to a full node. Thus, when nodes become full, special treatment must be used to avoid overfilling these nodes.

A means to effectively deal with this situation is rather straightforward when the finite element model is viewed as a collection of 1-D links. Then, only the flow of hydrogen between two nodes needs to be considered for each link. The way to achieve this is to cut the link in half and assume that the v_s in each half is constant at the nodal v_s in each half (figure 3.2.2). If these two halves are reconnected, the link is essentially defined by two conducting elements in series. By simple circuit theory, or by condensing out an internal node where the two halves of the link connect, a new link stiffness

$$k_{link} = \frac{2v_{s1}\, v_{s2}\, \bar{k}_{link}}{v_{s1} + v_{s2}} \begin{bmatrix} 1 & -1 \\ -1 & 1 \end{bmatrix}$$

is obtained where $\bar{k}_{link}$ is the link stiffness when $v_{s1} = v_{s2} = 1$ (no precipitate). This stiffness has the property that if v_s at either node becomes zero, the stiffness becomes zero (the link is effectively removed) and no more hydrogen can diffuse into the full node. If v_s at a node becomes zero, all links to that node are for numerical purposes eliminated. In practice, v_s never actually becomes exactly zero but rather it asymptotically approaches zero. This means that the links will never be completely severed and in the event of a change in thermal conditions, dissolution of hydrogen that would remove hydrogen from a full (nearly full) node can take place in the finite element model.

3.2.3 *Nonlinear Coupled Thermal/Hydrogen Diffusion Analysis*

Any analysis involving hydrogen diffusion is assumed to be transient since steady state situations are of little practical use. The basic procedure for obtaining a transient solution is the same as the explicit integration method used in thermal analysis where the stiffness is multiplied with the nodal variables at the element level and the resulting load vectors are then assembled. The main difference between hydrogen diffusion analysis and thermal analysis is the need for the TSS algorithm to determine the concentration in solution. This algorithm does not interfere with the basic explicit integration scheme since it is applied separately at the end of each time step.

One feature of hydrogen diffusion and precipitation is that certain thermal histories have a profound effect on the evolution of concentration distribution. In addition, the concentration distribution can have a significant effect on thermal properties and boundary conditions. Thus there exists a coupling between temperature and concentration:

Concentration depends on temperature through:

1) thermal driving force
2) material properties
3) TSS hysteresis due to cyclic temperature changes

Temperature depends on concentration through:

1) material properties
2) boundary conditions/contact condition

The present finite element model used with the TSS model considered herein is capable of modelling the hysteresis effects caused by repeated increasing and decreasing of temperature fields. Therefore, in a general transient analysis, there must be a provision to change the thermal field at specified intervals, either because of imposed temperature changes (due to operating conditions) or because of the interaction of the evolving concentration distribution with thermal properties. The basic approach to this is:

1) start with an initial thermal field and perform the hydrogen diffusion analysis until enough precipitate is present to affect thermal boundary conditions. Then, perform a new thermal analysis to be used until a further increase in precipitate affects thermal boundary conditions, etc.;

2) perform hydrogen diffusion analysis until time is reached to impose specified thermal conditions (operating condition). Then, perform TSS logic and or hydrogen diffusion analysis until time to change the thermal field again.

This approach is potentially complicated but some simplification is obtained since the same geometric model can be used for both thermal and hydrogen diffusion analysis. At the start of a new thermal cycle, new elemental stiffness matrices must be formed based on the new temperature values. With the link representation of elements, this can be achieved by simply adjusting previous link stiffnesses. Also, the nodal concentrations must be renormalized with equation 3.2.2 in accordance with the new thermal field. A flowchart showing the main organization of coupled thermal/hydrogen diffusion analysis is given in figure 3.2.3.

In view of the relative magnitudes of thermal diffusivity and hydrogen molecular diffusivity, the temperature field is assumed to reach steady state instantaneously upon the application of new thermal boundary conditions. At the instant that a new thermal field is applied, the amount of concentration in solution must be constrained to comply with the TSS defined by the new thermal field. The total concentration is assumed to remain constant while the new thermal field is imposed. The logic to adjust concentration in solution to comply with the thermal history is:

1) Temperatures decreasing

   i) if $c_s^{old} > TSSP^{new}$ then $c_s^{new} = TSSP^{new}$

   ii) otherwise $c_s^{new} = c_s^{old}$

2) Temperatures increasing

   i) if $c_s^{old} < TSSD^{new}$ then $c_s^{new} = \min(c, TSSD^{new})$

   ii) otherwise $c_s^{new} = c_s^{old}$

Note that, here normalized concentration and TSS values are not used because the normalization factors change when temperatures change.

4.0 ELEMENT REPRESENTATION

4.1 Isoparametric Continuum Elements

The isoparametric continuum elements are all based on linear shape functions and all have just one degree of freedom per node. The stiffness, capacitance, and source matrices for either thermal or molecular diffusion are determined by a standard application of Galerkin's method to the governing differential equation, (3.1.1) or (3.2.3). The lumped capacitance matrix used in the program is obtained by summing the columns of the consistent capacitance so that the total coincides with the volumetrically calculated capacitance. The necessary expressions are:

$$[K] = \int_v [B]^T [k] [B] \, dV \tag{4.1.1}$$

$$[m_{ij}] = \sum_j \int_v \rho c \{N_i\} [N_j] \, dV \tag{4.1.2}$$

$$\{R_Q\} = \int_v Q \{N\} \, dV \tag{4.1.3}$$

where $\{N_i\}$ is a vector of shape functions.

A routine but more thorough derivation is presented in [3]. Here, just the main points regarding the element formulations are stated without derivations.

4.1.1 *1-D Continuum Element*

The one dimensional continuum element shown in figure 4.1.1a and 4.1.1b has two degrees of freedom and utilizes linear shape functions. The data defining the element is:

- x, y, and z coordinates of both nodes
- cross-sectional area (constant over length)
- material number

For constant material properties and cross-section, the elemental stiffness and lumped capacitance for cartesian coordinates are given directly by

$$[K] = \frac{kA}{L} \begin{bmatrix} 1 & -1 \\ -1 & 1 \end{bmatrix} \tag{4.1.4}$$

$$[M] = \frac{\rho c L A}{2} \begin{bmatrix} 1 & 0 \\ 0 & 1 \end{bmatrix} \tag{4.1.5}$$

$$\{R_Q\} = \frac{QLA}{2}\begin{Bmatrix}1\\1\end{Bmatrix} \tag{4.1.6}$$

Axisymmetric problems are treated by using the first two coordinates, x and y, to represent r and z, respectively. The resulting matrices are:

$$[K] = \frac{\pi k t(r_1 + r_2)}{L}\begin{bmatrix}1 & -1\\-1 & 1\end{bmatrix} \tag{4.1.7}$$

$$[M] = \frac{\pi \rho c t L}{3}\begin{bmatrix}2r_1 + r_2 & 0\\0 & r_1 + 2r_2\end{bmatrix} \tag{4.1.8}$$

$$\{R_Q\} = \frac{\pi QtL}{3}\begin{Bmatrix}2r_1 + r_2\\r_1 + 2r_2\end{Bmatrix} \tag{4.1.9}$$

4.1.2 *2-D Continuum Element*

The two dimensional isoparametric continuum element is evaluated by numerically integrating (Gauss-Legendre quadrature) equations (4.1.1) to (4.1.3) above. Element properties are interpolated at Gauss points while performing the integrations. The data required to define a 2-D element is

- x, y, and z coordinates for four nodes
- thickness
- material number

The node numbering order is indicated in figure 4.1.1c and 4.1.1d. An axisymmetric version of 2-D continuum element uses only the first two coordinates, x and y, to define r and z, respectively.

4.1.3 *3-D Continuum Elements*

The three dimensional isoparametric continuum element is determined in a similar manner to the 2-D element. In computing the element matrices, equations (4.1.1) to (4.1.3) are evaluated by interpolating element values at integration points. A modified formulation of the 3-D continuum element, based on one point quadrature formulations [7,8], is used for coupled thermal/hydrogen diffusion analyses. A complete description is given in Appendix B.

The data required to define a 3-D element is

- x, y, and z coordinates for eight nodes
- material number

The node numbering order is indicated in figure 4.1.1e. There can be no axisymmetric version of a 3-D element.

4.1.4 *Boundary Conditions*

There are three basic types of boundary conditions that can be specified in H3DTAP:

i) distributed flux on surface
ii) concentrated source at a node(s)
iii) specified temperature/concentration at a node(s)

Figure 4.1.2 depicts the various ways in which these boundary conditions may appear. The distributed heat flux boundary condition is handled by computing the consistent load vector from

$$\{R_q\} = \int_A q_s \{N\}\, dA \tag{4.1.10}$$

where {N} is the vector of shape functions.

A distributed load can be applied to the

i) length of a 1-D element or edge of a 2-D element
ii) surface of a 2-D or 3-D element

In case (i) the two nodes defining the edge are specified along with a value for q which must represent the flux density per unit length. The load vector is given by

$$\{R_q\} = \frac{qL}{2}\begin{Bmatrix}1\\1\end{Bmatrix} \tag{4.1.11}$$

or for axisymmetric problems

$$\{R_q\} = \frac{\pi qL}{3}\begin{Bmatrix}2r_1 + r_2\\ r_1 + 2r_2\end{Bmatrix}$$

Note that for axisymmetric problems, q must represent flux density per unit area.

For case (ii) four nodes define the surface and q is the flux density per unit area. The area of the surface is computed from the coordinates of the four nodes given and the load vector is

$$\{R_q\} = \frac{qA}{4}\begin{Bmatrix}1\\1\\1\\1\end{Bmatrix} \tag{4.1.13}$$

Note that if the problem is axisymmetric, there can be no surface flux applied to the surface of a 2-D element, only to the edge. This method of determining the load vector requires that the surfaces should be as rectangular as possible to minimize discretization error.

Concentrated heat sources can be applied to any node by simply adding the value of the concentrated source to the entry of the load vector corresponding to the specified node.

The application of specified temperature boundary conditions is done in the following way.

i) for static problems and linear implicit transient problems, set K_{ii} to 10^{30} and the load vector to $10^{30}*T_{spec}$ for the specified node

ii) for explicit nonlinear problems, at the end of each time step, set the specified nodal values to their respective specified temperatures.

4.2 Contact Elements

4.2.1 *General Derivation*

The manner in which convection boundary conditions are treated in H3DTAP is somewhat different than the usual approach. The main difference is that the ambient space is included in the model and an element is defined having the same conductive properties as the convective boundary condition. In other words, the conducting medium is connected to ambient space by a fictitious material that models convection conductance. The same basic approach is used for modelling radiation boundary conditions but for incident radiation between surfaces, view factors must be incorporated. Presently, only special cases of radiation can be handled since there is no view factor algorithm in H3DTAP.

Consider convection from the surface shown in figure 4.2.1 defined by r nodes (r=4 in figure 4.2.1a). Also consider that this surface element has two sides, side A is the conduction side and side B is the ambient side. In general, the temperature on the conducting side and the temperature on the ambient side varies with position. According to the usual mathematical model of convective heat transfer, the heat flux per unit area through the surface (from side A to side B) is

$$q(x) = h\left(T_A(x) - T_B(x)\right) \tag{4.2.1}$$

where q(x) is the flux which also varies with position. Application of the method of weighted residuals to equation (4.2.1) gives

$$\int_A N_i(x)\left[\, h \sum_j N_j(x)\left(T_{A_j} - T_{B_j}\right) - q(x)\right] dA = 0 \tag{4.2.2}$$

The above integral defines a matrix equation

$$\left[\, K_{ij}^h \,\right]\left\{\, T_{A_j} - T_{B_j} \,\right\} = \left\{\, q_i \,\right\} \tag{4.2.3}$$

where

$$K_{ij}^h = \int_A h\, N_i N_j\, dA \tag{4.2.4}$$

$$q_i = \int_A N_i q \, dA \tag{4.2.5}$$

Now consider the same element but with 2r nodes; node i is coincident with node i+r. In a new notation, the temperature on the conducting side is $(T_A)_i = T_i$ and the temperature on the ambient side is $(T_B)_i = T_{i+r}$. Thus equation (4.2.3) is

$$\left[K_{ij}^h\right] \{ T_j - T_{j+r} \} = \{ q_i \} \tag{4.2.6}$$

which can be written in an augmented matrix form

$$\left[K_{ij}^h \mid -K_{ij}^h \right] \begin{Bmatrix} T_j \\ - - - \\ T_{j+r} \end{Bmatrix} = \{ q_i \} \tag{4.2.7}$$

Suppose that nodes i and i+r are not coincident but are separated by some distance as shown in figure 4.2.1b. Then the consistent heat flow out of node i must go into node i+r so that

$$q_i = -q_{i+r} \tag{4.2.8}$$

This allows equation 4.2.7 to be further augmented to

$$\begin{bmatrix} K_{ij}^h & \mid & -K_{ij}^h \\ - - - & - & - - - \\ -K_{ij}^h & \mid & K_{ij}^h \end{bmatrix} \begin{Bmatrix} T_j \\ - - - \\ T_{j+r} \end{Bmatrix} = \begin{Bmatrix} q_i \\ - - - \\ q_{i+r} \end{Bmatrix} \tag{4.2.9}$$

which shows a 2r by 2r stiffness matrix for the entire element. This stiffness matrix represents the conductivity of an imaginary material with a thermal resistance that is independent of thickness. The three versions of this element are shown in figure 4.2.2.

To model a convection boundary condition, attach nodes 1 to r of this element to the surface of the conducting body and specify the ambient temperature on nodes r+1 to 2r on the contact element. It should be noted that this formulation is equivalent to the convection formulation in [3] although the form of the equations is different, and additional nodes are required to specify the ambient temperature. Some computational efficiency is gained by using a lumped form of $[K^h]$ obtained by summing the columns of the consistent $[K^h]$ to form a diagonal matrix in the same way a diagonal lumped capacitance matrix is obtained in equation (4.1.2).

From the augmented form of the contact element stiffness matrix, it should be clear that the first r nodes and their coordinates completely define the element properties, and the remaining nodes can be positioned arbitrarily when modelling convection to ambient space. In fact, if ambient temperature is uniform, nodes r+1 to 2r can all be given one common node number; the temperature of this common node must then be set to ambient temperature.

The contact element is also useful for modelling thermal contact resistance between two conducting bodies. In the case of thermal contacts, the ambient side of the element has nodes that belong to an additional conducting body. The coordinates of the ambient side nodes must be either coincident with the corresponding nodes on the conducting side, or they must be uniformly displaced so that the surfaces on both conducting bodies that are connected by the contact element are congruent.

4.2.2 *1-D Contact Element*

The one dimensional contact element is trivial in its derivation since the shape function is equal to unity. Thus equation (4.2.4) yields

$$K_{11}^{h} = hA \tag{4.2.10}$$

and the entire element stiffness is

$$[K] = hA \begin{bmatrix} 1 & -1 \\ -1 & 1 \end{bmatrix} \tag{4.2.11}$$

Note that this stiffness is the same as for a 1-D continuum element of length and conductivity such that k/L = h.

4.2.3 *2-D Contact Element*

For two dimensional contact elements, r=2 in the notation of section 4.2.1. Equation (4.2.4) defining the stiffness can be integrated in closed form when the width of the surface does not vary along the length of the element. The result is

$$[K^{h}] = \frac{hLt}{6} \begin{bmatrix} 2 & 1 \\ 1 & 2 \end{bmatrix} \tag{4.2.12}$$

Axisymmetric contact elements have the width of surface proportional to the radius so equation (4.2.4) yields

$$[K^{h}] = \frac{hL}{12} \begin{bmatrix} 3x_1 + x_2 & x_1 + x_2 \\ x_1 + x_2 & x_1 + 3x_2 \end{bmatrix} \tag{4.2.13}$$

The complete stiffness matrix is obtained as the augmented matrix given by equation 4.2.9. The node numbering scheme given in figure 4.2.2 is essentially the same as for 2-D continuum elements. However, here care must be taken to ensure that nodes 1 and 2 are on one side of the contact and that nodes 3 and 4 are on the other side.

4.2.4 *3-D Contact Element*

The three dimensional contact element is computed by numerical integration of equation (4.2.4). The result of this is augmented as per equation (4.3.9) to provide the complete stiffness matrix. Node numbering shown in figure 4.2.3 is the same as for 3-D continuum elements but again the first four and the last four nodes must consistently define each side of the contact. The 3-D contact element cannot be used in axisymmetric problems.

4.2.5 *Gap Dependent Contacts*

Contact elements that utilize a convective heat transfer coefficient are completely defined by the first half of the nodes defining the element. A situation can exist where two contacting bodies are connected thermally by conduction through a gap filled with a conducting material as shown in figure 4.2.3. For a given gap separation, x_g, this condition can be modelled by choosing a contact conductance of $h = k_g / x_g$.

In H3DTAP, there is an option that allows for automatic computation of h based on the actual separation of the contacting bodies. The two sides of the contact must have a finite separation to use this option. The main advantage in using contact elements for this situation rather than continuum elements is that for very small gaps, use of continuum elements results in an extremely small critical time step,

$$\Delta t_{cr} \leq \frac{(\Delta x_g)^2}{2(k/\rho c)_g} \tag{4.2.14}$$

whereas use of contact elements results in a time step,

$$\Delta t_{cr} \leq \frac{(\Delta x_e)^2}{2(k/\rho c)_e \left(1 + \dfrac{k_g}{k_e}\dfrac{\Delta x_e}{\Delta x_g}\right)} \tag{4.2.15}$$

depending more on the size of elements in the conducting body. In equations (4.2.14) and (4.2.15), the subscripts g and e indicate properties for the gap material and element material respectively. In many cases, equation (4.2.15) permits the use of much larger time steps than equation (4.2.14).

5.0 CONCLUDING REMARKS

Three major advantages of having computer programs such as H3DTAP and its structural analysis counterpart, H3DMAP, are:

1) specialization - ability to model highly specialized phenomena not addressed by commercial software.

2) efficiency - ability to obtain solutions with minimal cost, or alternatively to handle larger models.

3) flexibility - ability to incorporate new methods or mathematical models into the code to improve efficiency or to increase the scope of analysis of the program.

Experience gained so far in the use of H3DTAP confirms that all three of these advantages are actually realized. Recent modelling of hydride blister formation in Pickering NGS, Unit 4 fuel channels represents the state-of-the-art in non-linear transient simulation with distributed phase changes in 3-D. Commercial software is not capable of modelling the features of this specialized problem, so a code like H3DTAP is required. Also, the high efficiency of H3DTAP makes it feasible to run non-linear simulations with over 10,000 3-D elements undergoing transient response involving 500,000 time steps. One example of a finite element model used in this type of analysis [9] is shown in figure 5.1 and a sample of the temperature distribution in the area of pressure tube/ calandria tube contact is given in figure 5.2. Note that the tubes have been separated to facilitate visualization. Such large scale analyses are impractical using commercial scale programs on the relatively modest hardware available to run H3DTAP (i.e. μVAX mini computer, DEC 3100, DEC 5000, Hewlett Packard and Silicon Graphics workstations). Also H3DTAP can be easily adapted to PC's with 386 and 486 processors. In the course of doing fuel channel analyses, new numerical methods were developed to increase efficiency and to improve the accuracy of modelling phase change boundaries. These new methods, now incorporated in H3DTAP, are examples of how the flexibility of an in-house code offers significant advantages in modelling complex phenomena.

Future projects involving new mathematical models are expected to exploit the flexibility of H3DTAP and H3DMAP even further. For instance, work is underway to link these two programs to permit concurrent stress and diffusion analysis necessary to model the process known as delayed hydride cracking (DHC). This is one more example of a specialized problem requiring several modelling features that are unavailable in existing analysis codes. Thus, the enhancements made to accommodate this problem will advance the state-of-the-art to yet a higher level, and will increase the ability to assess the structural integrity of fuel channels and other components.

ACKNOWLEDGMENTS

Portions of this work, related specifically to hydrogen diffusion modelling, received funding from the CANDU Owners Group (COG). The author is most grateful for this support and the opportunity it provided to extend the application of analysis methods to new and important problems.

During the preparation of this report, many useful comments and suggestions were offered by Dr. T.P. Byrne and Mr. R.G. Sauvé. For this, as well as the skill and dedication of Mrs. C. Robshaw in typing the report, the author wishes to express his appreciation.

Approved by:

G.J. Clarke
Manager
Mechanical Research Department

Submitted by:

D.R. Metzger
Engineer
Applied Mechanics Section

Reviewed by:

R.G. Sauvé
Unit Head-Applied Mechanics Development
Applied Mechanics Section

REFERENCES

1. Sauvé, R.G., *"H3DMAP Version 3, Three Dimensional Matrix Analysis Program for Structures, Theoretical Manual, Volumes 1 and 2"*, Ontario Hydro D&D Report No. 87419, October 1987.

2. Sauvé, R.G., Nadeau, E., *"H3DMAP Version 4, A General Three Dimensional Finite Element Computer Code for Linear and Non-Linear Analysis of Structures: User Manual and Verification Cases, Vols. 1 and 2"*, Ontario Hydro Research Division Report No. 89-221-K, October 1989.

3. Heubner, K.H., Thornton, E.A., *"The Finite Element Method for Engineers"*, John Wiley and Sons, 1982.

4. Metzger, D.R., *"Network Model for Explicit Time Integration of Finite Element Diffusion Equations"*, Transactions, SMiRT 11, Japan, 1991.

5. Byrne, T.P., *"Hydride Precipitation and Blister Growth Modelling in Zr-Nb Pressure Tubes - Progress Report No. 1"*, OHRD Report No. 84-30-H, February 1984.

6. Byrne, T.P., Leger, M., *"Hydride Blister Growth Modelling - Progress Report No. 2"*, OHRD Report No. 85-29-H, September 1985.

7. Liu, W.K., Belytschko, T., *"Efficient Linear and Nonlinear Heat Conduction with a Quadrilateral Element"*, International Journal for Numerical Methods in Engineering, Vol. 20, pp. 931-948, 1984.

8. Belytschko, T., Ong, J.S., Liu, W.K., Kennedy, J.M., *"Hourglass Control in Linear and Nonlinear Problems"*, Computer Methods in Applied Mechanics and Engineering, Vol. 43, pp. 251-276, 1984.

9. Byrne, T.P., Metzger, D.R., Leger, M., *"The Application of Zirconium Hydride Blister Modelling to the P2-G16 Failure"*, OHRD Report No. 91-126-K, 1991.

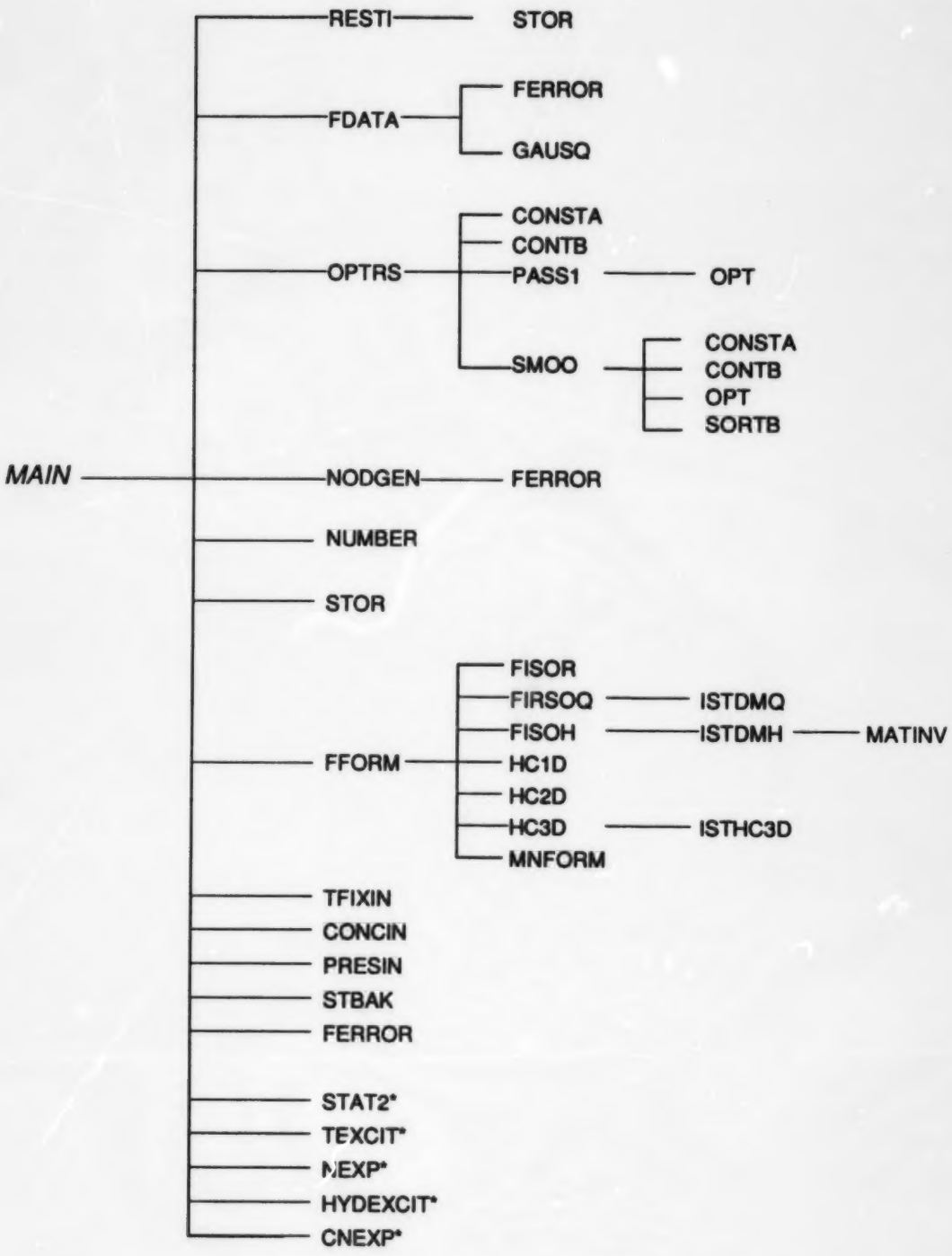

* Indicates Analysis Modules

FIGURE 2-1

TREE STRUCTURE OF MAIN PROGRAM

91-102-K

185476-B30-I

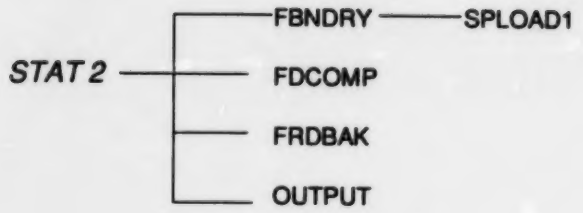

(a) Linear Steady-State Heat Transfer

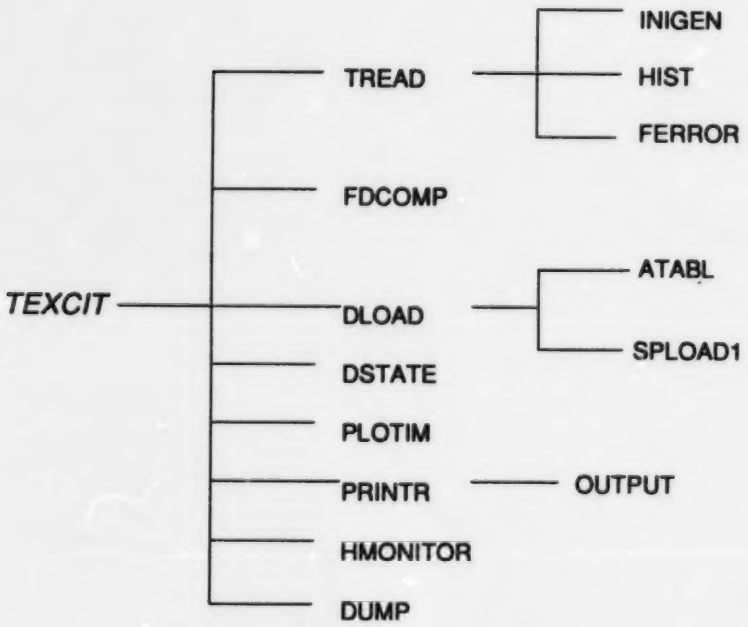

(b) Linear Implicit Transient Heat Transfer

FIGURE 2.2

TREE STRUCTURE OF ANALYSIS MODULES

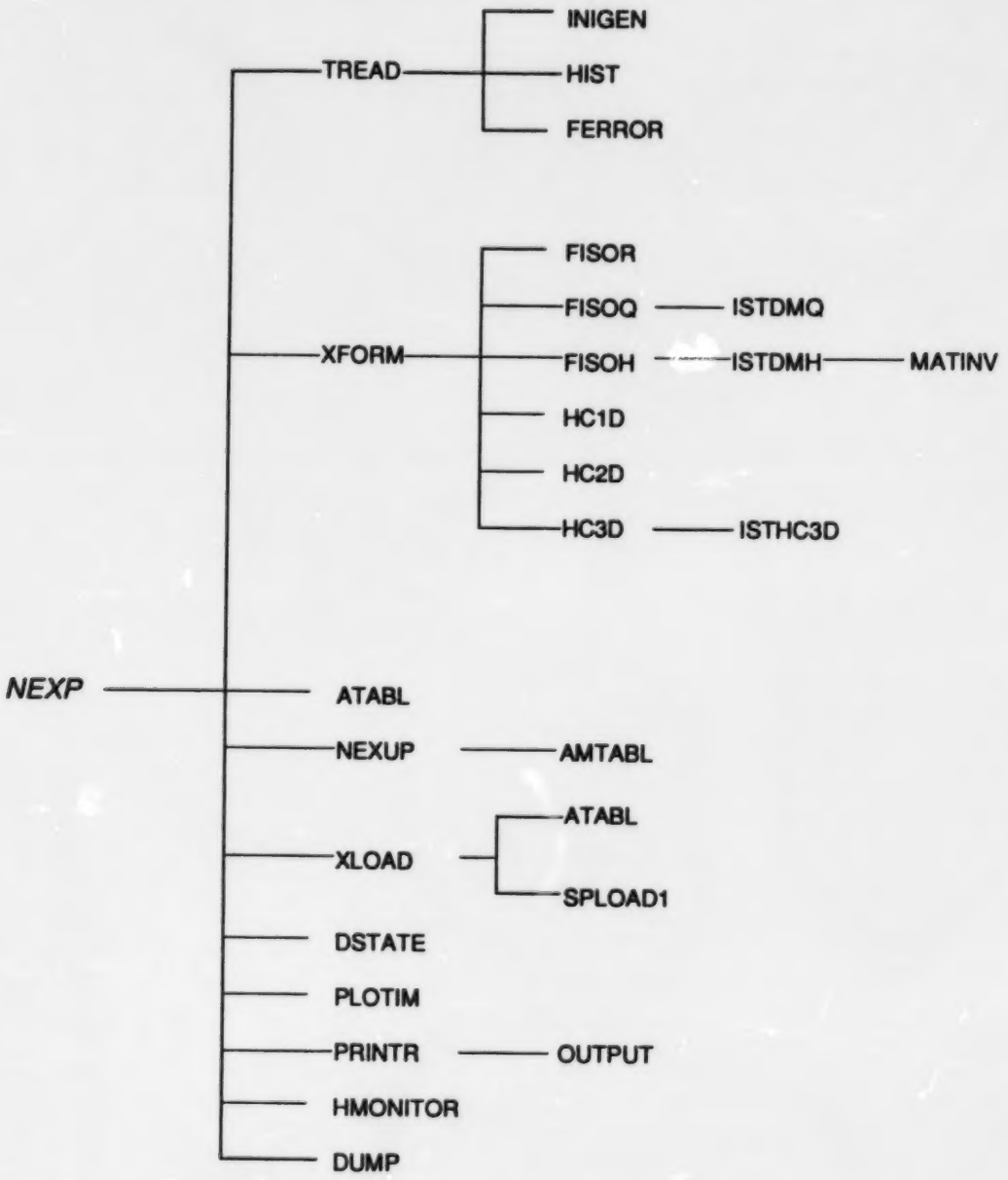

(c) Nonlinear Explicit Transient Heat Transfer

FIGURE 2.2

TREE STRUCTURE OF ANALYSIS MODULES

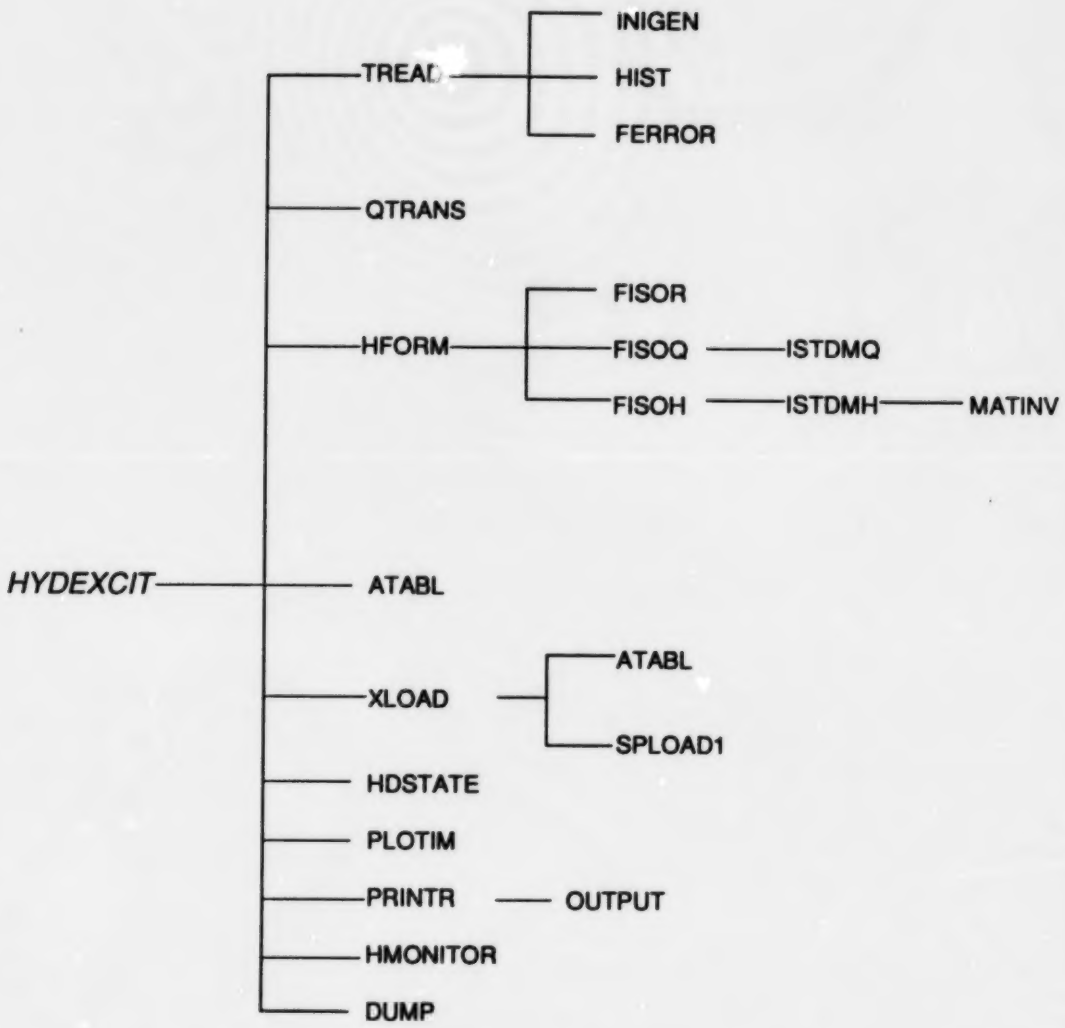

(d) Constant Temperature Hydrogen Diffusion

FIGURE 2.2

TREE STRUCTURE OF ANALYSIS MODULES

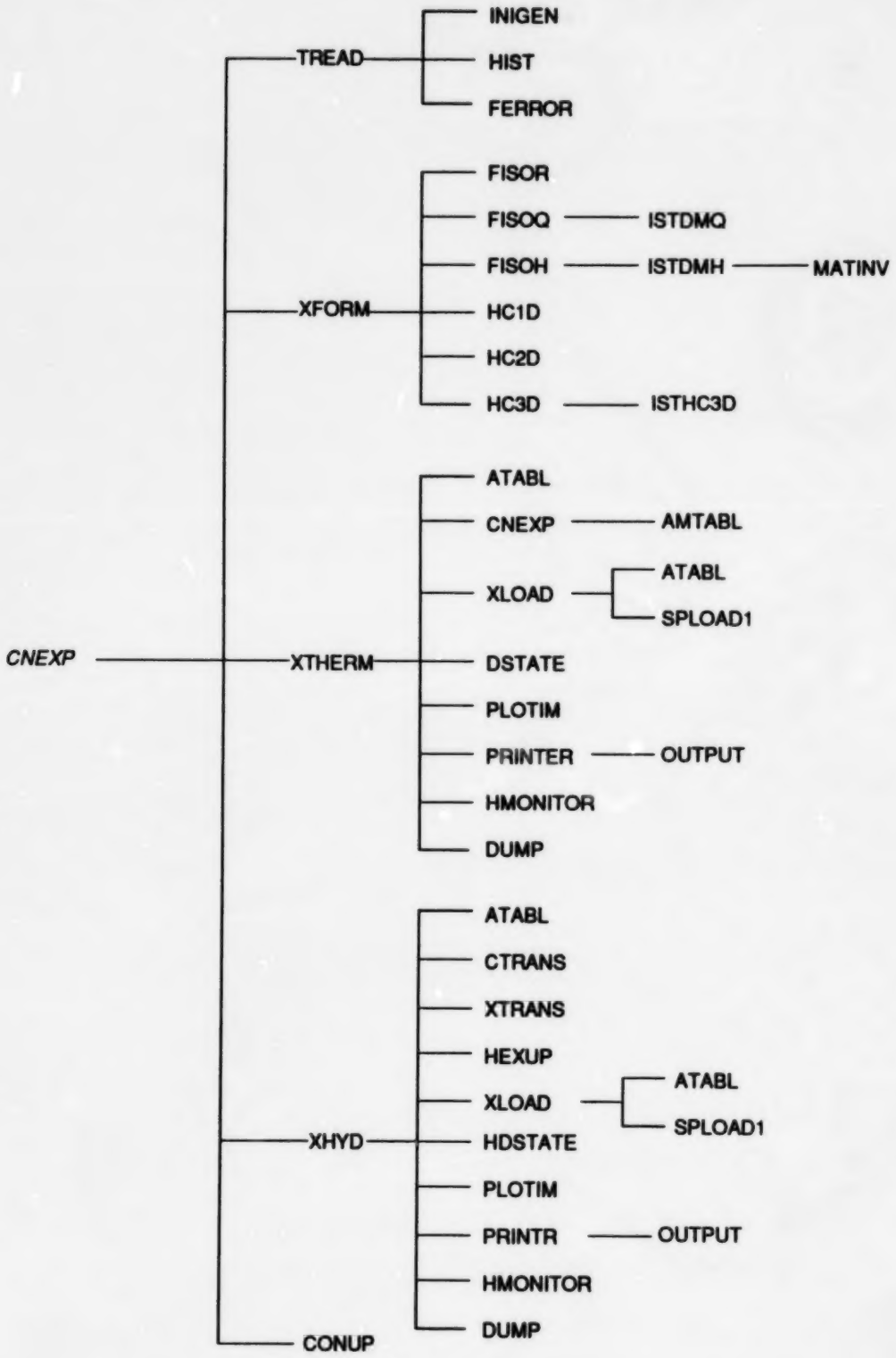

(e) Coupled Heat Transfer/Hydrogen Diffusion analysis

FIGURE 2.2

TREE STRUCTURE OF ANALYSIS MODULES

91-102-K
185480-B31-RD

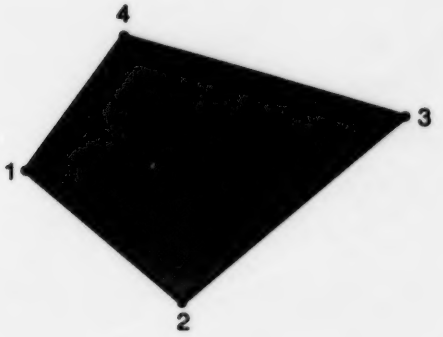

Continuum Element

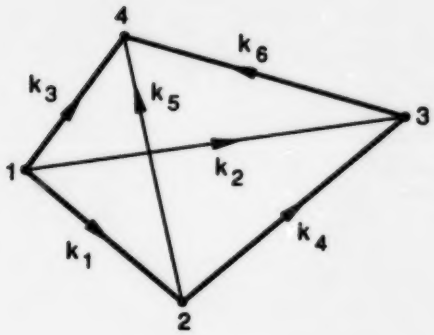

Network Representation

$$K_e = \begin{bmatrix} k_1+k_2+k_3 & -k_1 & -k_2 & -k_3 \\ -k_1 & k_1+k_4+k_5 & -k_4 & -k_5 \\ -k_2 & -k_4 & k_2+k_4+k_6 & -k_6 \\ -k_3 & -k_5 & -k_6 & k_3+k_5+k_6 \end{bmatrix}$$

$$k_{link} = k_i \begin{bmatrix} 1 & -1 \\ -1 & 1 \end{bmatrix}$$

FIGURE 3.1.1

NETWORK REPRESENTATION OF CONTINUUM ELEMENT

91-102-K
185493-F26-RD

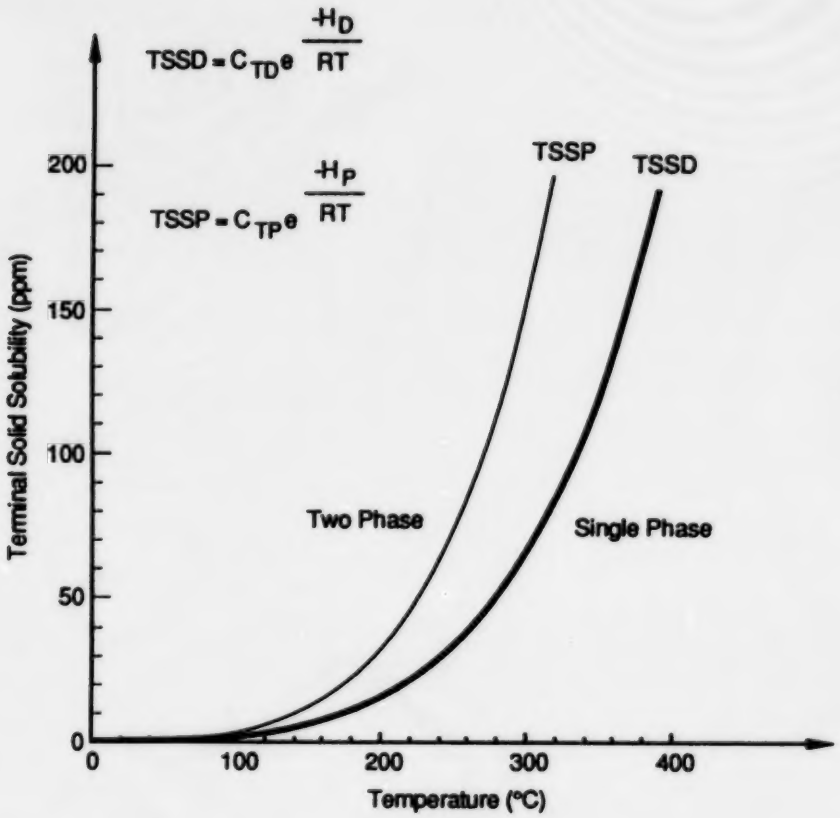

FIGURE 3.2.1

TEMPERATURE DEPENDENCE OF TERMINAL SOLID SOLUBILITY

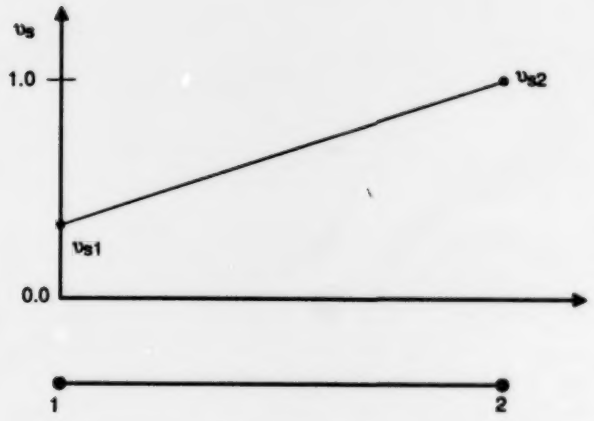

(a) Linear υ_s Distribution

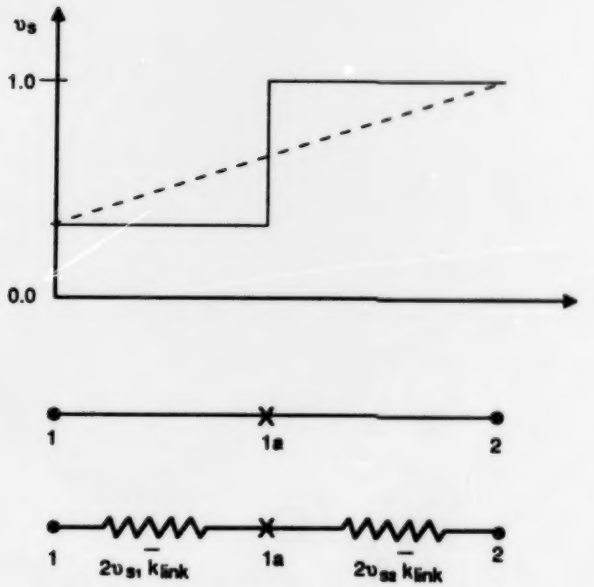

(b) Step Distribution of υ_s

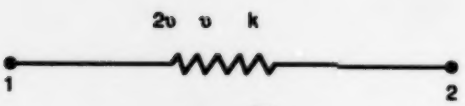

$$\frac{2\upsilon_{s1}\,\upsilon_{s2}\,\bar{k}_{link}}{\upsilon_{s1}+\upsilon_{s2}}$$

(c) Step Distribution Conductances in Series

FIGURE 3.2.2

MODELLING EFFECT OF PRECIPITATION ON ELEMENT PROPERTIES

91-102-K

185554-C21-R0

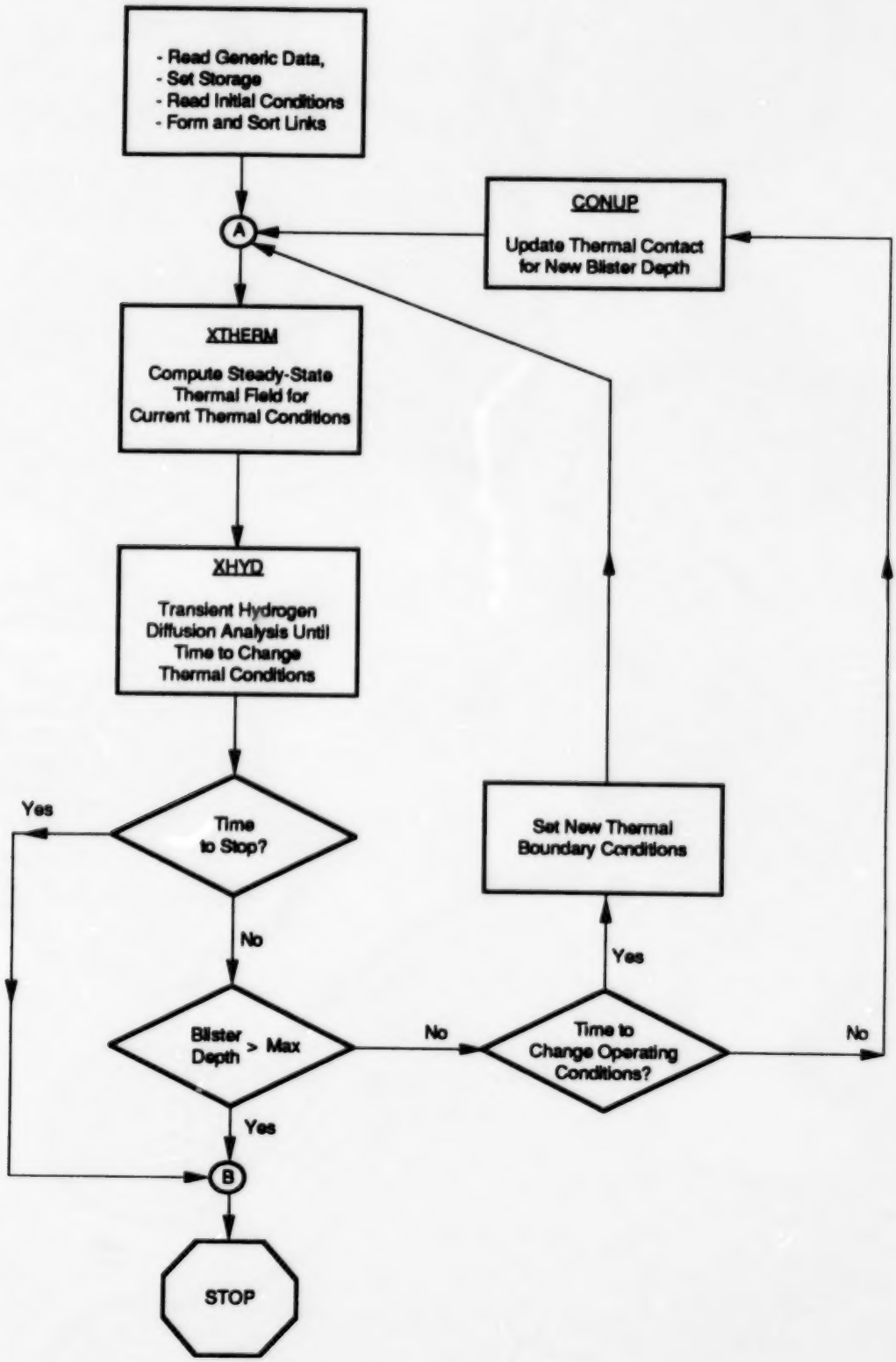

FIGURE 3.2.3

FLOWCHART OF COUPLED THERMAL/HYDROGEN DIFFUSION ANALYSIS

91-102-K
185488-E01-R1

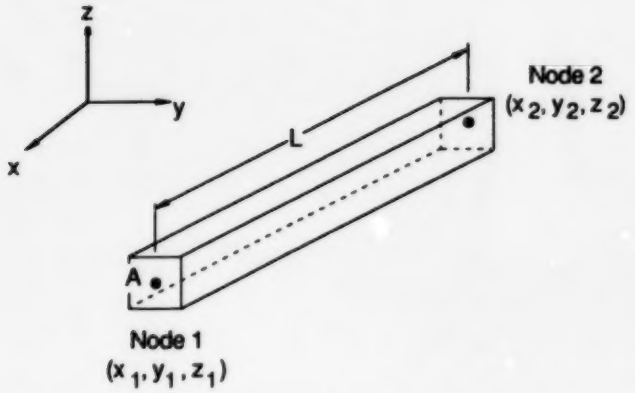

(a) 1-D Cartesian Element

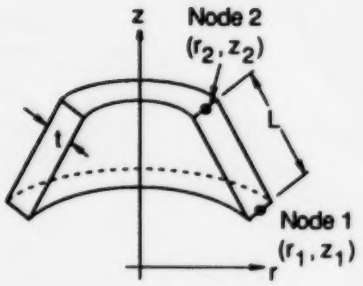

(b) 1-D Axisymmetric Element

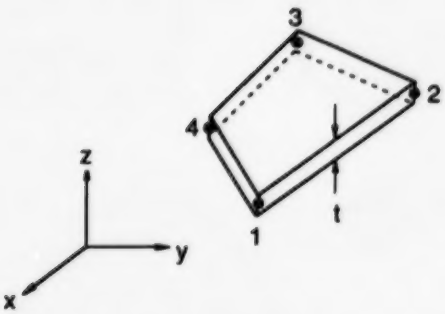

(c) 2-D Cartesian Element

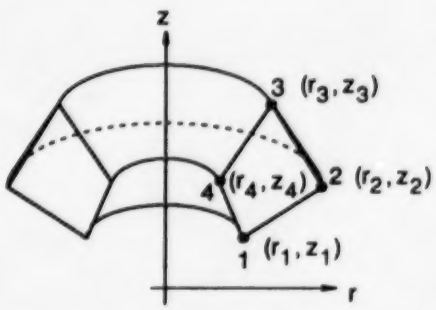

(d) 2-D Axisymmetric Element

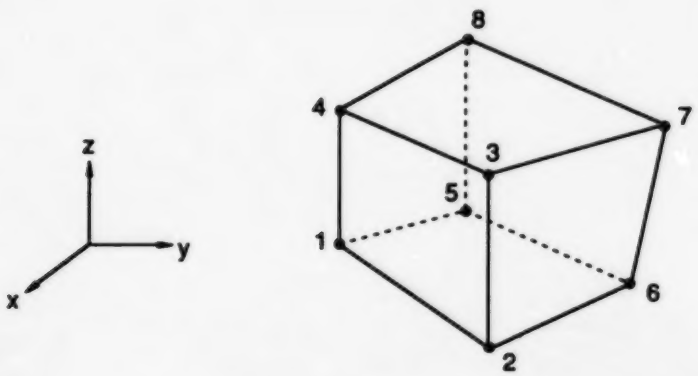

(e) 3-D Element

FIGURE 4.1.1

CONTINUUM ELEMENT NODE NUMBERING ORDER

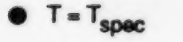

Specified Nodal Value

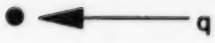

Concentrated Flux

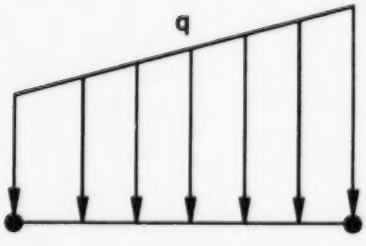

Distributed Flux

FIGURE 4.1.2

BOUNDARY CONDITIONS

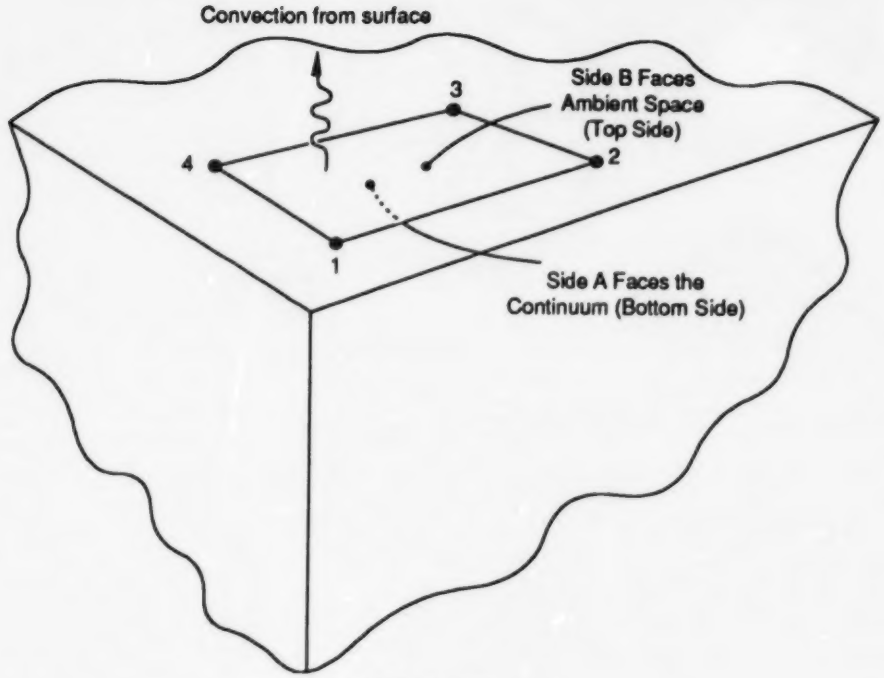

(a) Surface Element

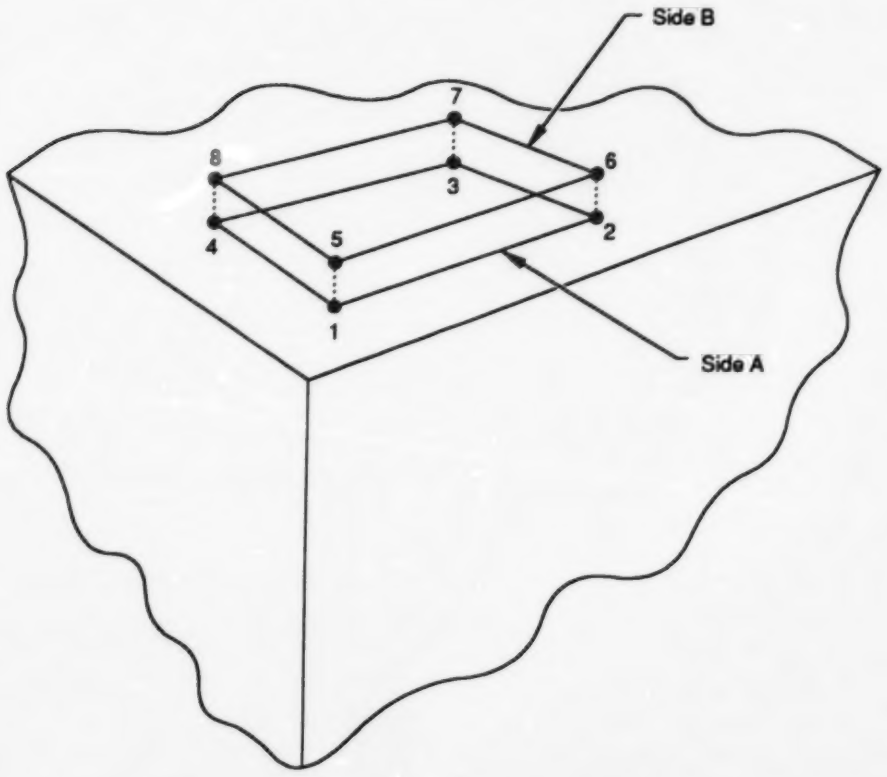

(b) Augmented Element to Include Ambient Space

FIGURE 4.2.1

CONVECTION FROM A SURFACE

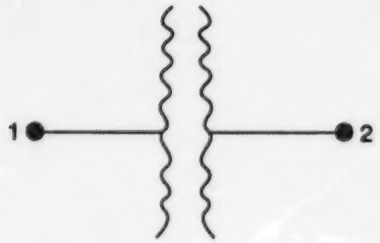

1-D

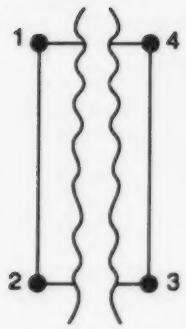

2-D

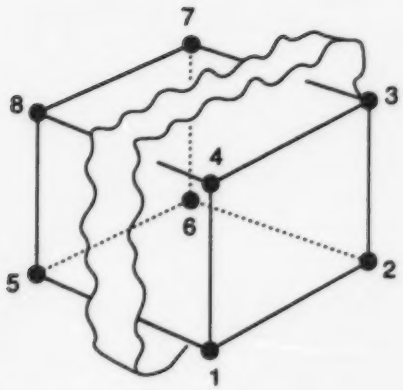

3-D

FIGURE 4.2.2

CONTACT ELEMENT NODE NUMBER ORDER

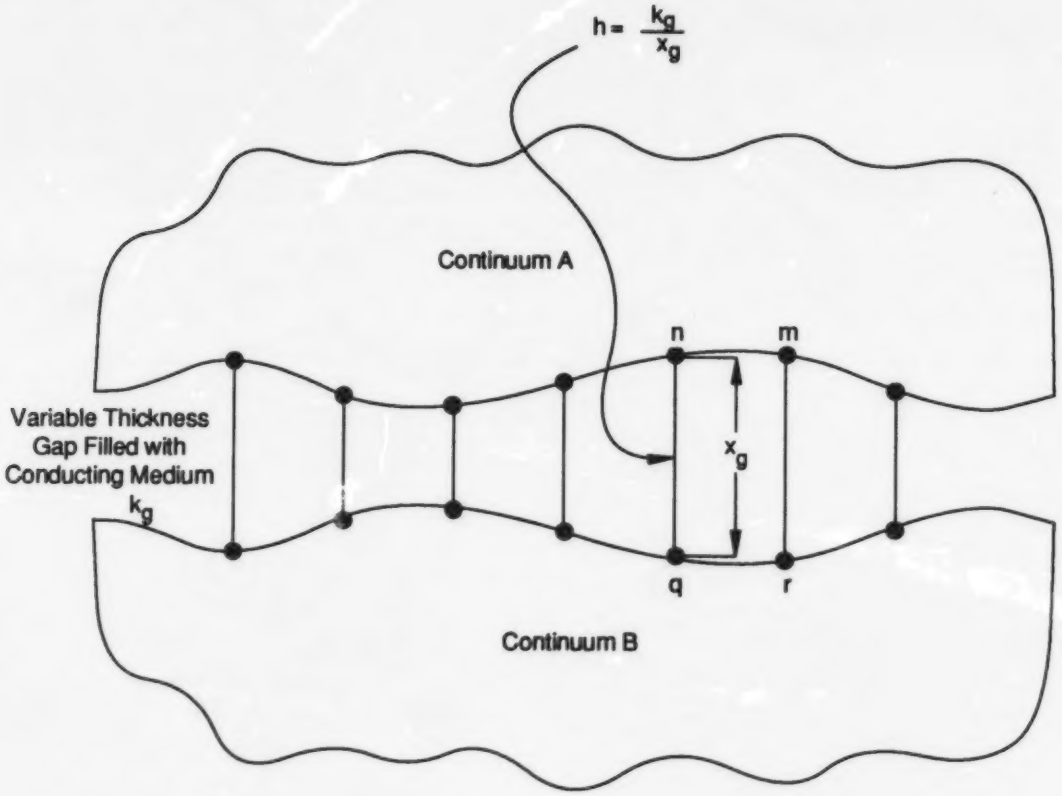

FIGURE 4.2.3

CONDUCTION THROUGH VARIABLE THICKNESS GAP

91-102-K
185494-F26-RD

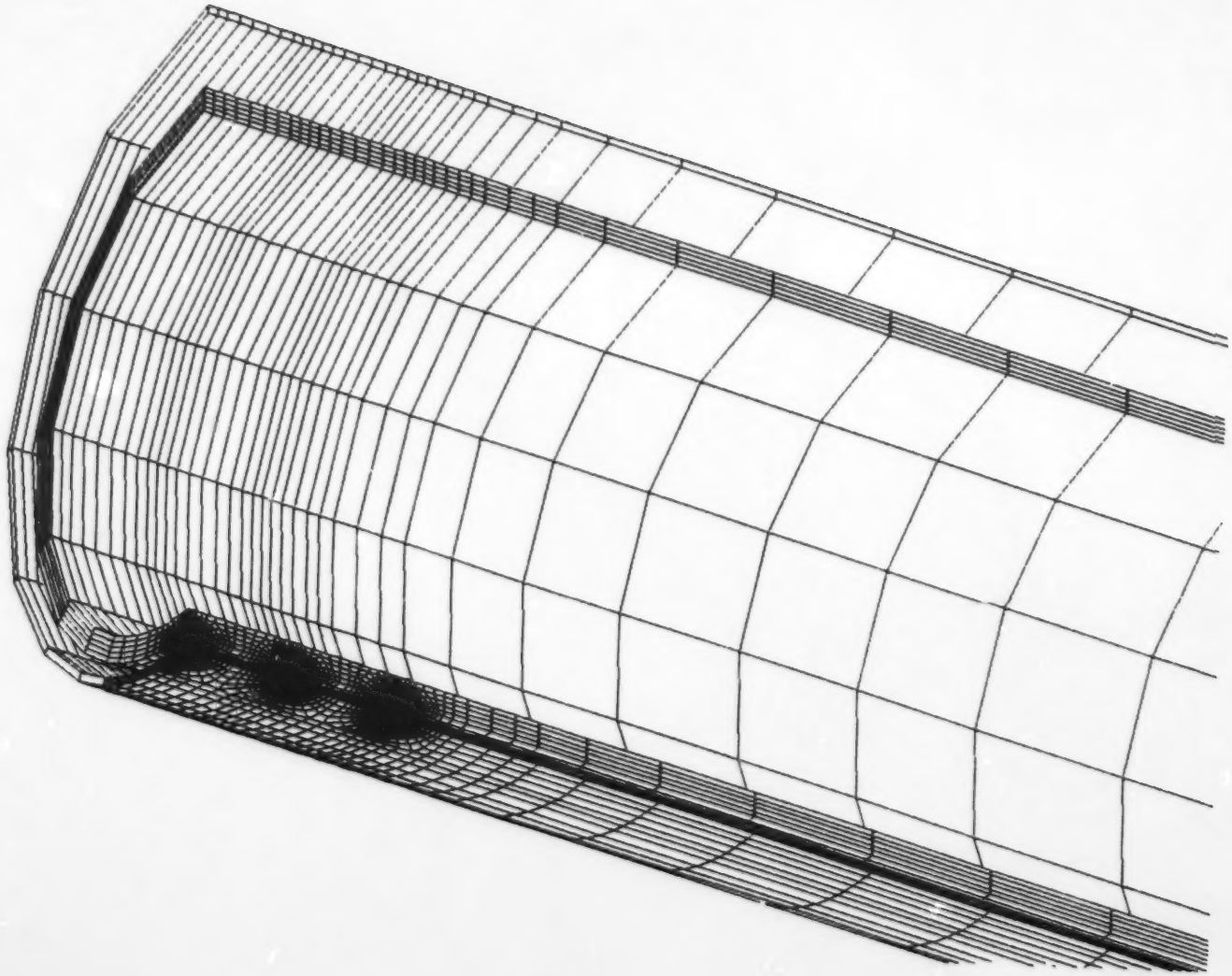

FIGURE 5.1

MESH FOR PICKERING UNIT 2 WITH MULTIPLE CONTACTS BETWEEN PRESSURE TUBE AND CALANDRIA TUBE

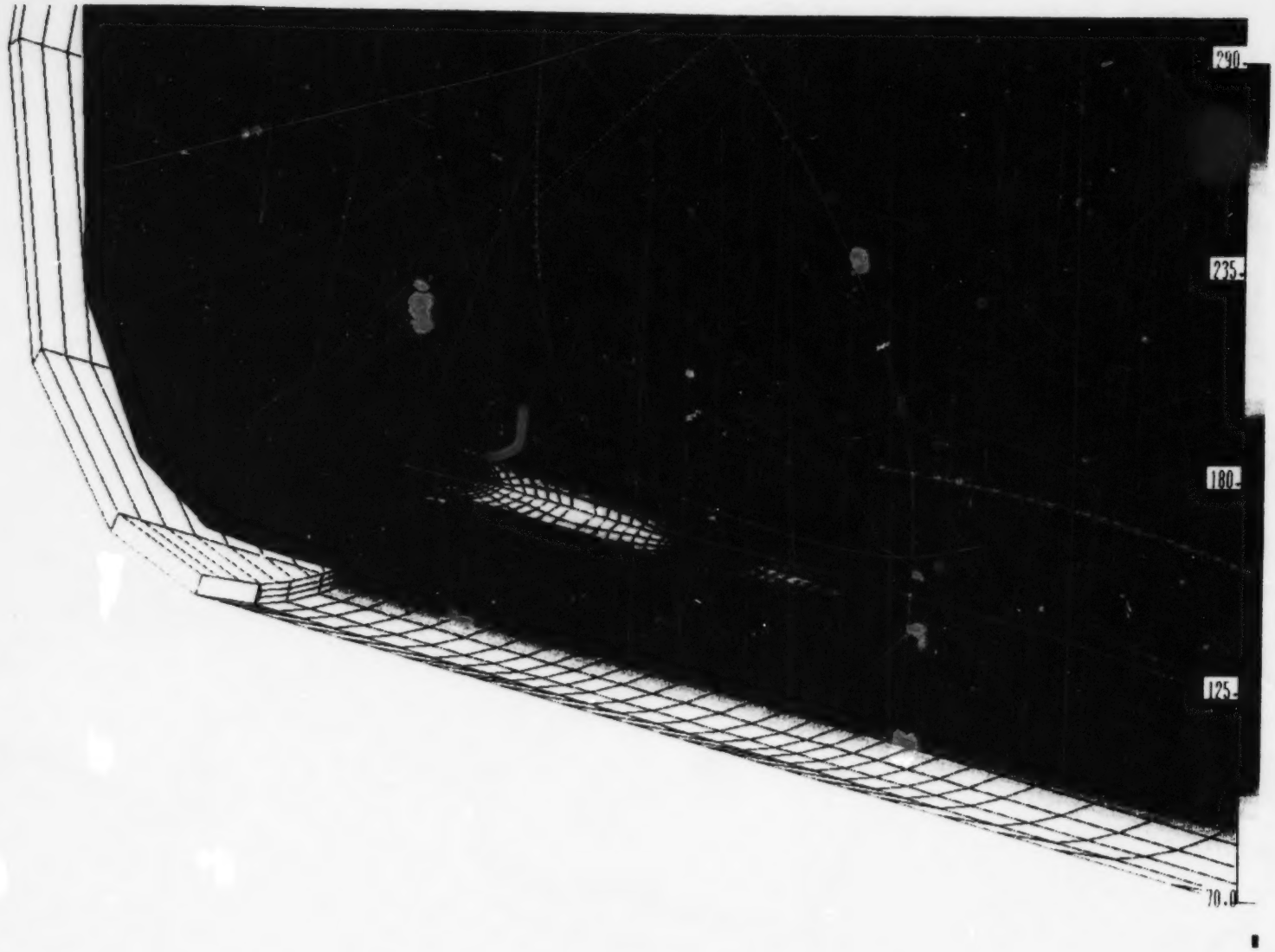

FIGURE 5.2

TEMPERATURE DISTRIBUTION IN P2 G16
FOR ONE 2.5 mm RADIUS CONTACT

APPENDIX A

USERS MANUAL (H3DTAP VERSION 1.0)

INPUT DATA FOR COMPUTER PROGRAM H3DTAP

RECORD 1: TITLE
FORMAT (40A2)

RECORD 2: NP,NROOT,LTFIX,LCONC,LPRES,LTYP,IAXI,INDOF(1)
FORMAT (8I7)

where:

NP	=	Number of nodes
NROOT	=	Flag for initial TSS logic (not enabled yet)
LTFIX	=	Number of nodes with specified nodal values
LCONC	=	Number of nodes with specified concentrated flux
LPRES	=	Number of imposed flux boundary surfaces
LTYP	=	1 for linear steady state heat transfer analysis
LTYP	=	2 for linear transient heat transfer (implicit)
LTYP	=	3 for nonlinear transient heat transfer (explicit)
LTYP	=	4 for transient hydrogen diffusion (explicit)
LTYP	=	5 for coupled thermal/hydrogen diffusion (explicit)
IAXI	=	Axisymmetric flag: 0 for Cartesian Coordinates 1 for Axisymmetric Coordinates
INDOF(1)	=	Master degree of freedom code (d.o.f.), 0=free, 1=fixed

Skip record 2A if LTYP is not equal to 5

RECORD 2A: NN2,LTFIXH,LCONCH,LPRESH
FORMAT(4I7)

where:

NN2	=	Number of nodes in hydrogen diffusion model
LTFIXH	=	Number of nodes in hydrogen diffusion model with specified concentration
LCONCH	=	Number of nodes in hydrogen diffusion model with specified concentrated source
LPRESH	=	Number of imposed flux surfaces in hydrogen diffusion model

RECORD 3: (IPRINT(I),I=1,6),IPLOT,(MODE(J),J=1,5)
(FORMAT (12I6)

where:

IPRINT(1)	=	(not used)
IPRINT(2)	=	1 for temperature/concentration output
IRPINT(3)	=	1 for concentration in solution
IPRINT(4)	=	1 for volume fraction of parent material
IPRINT(5)	=	(not used)
IPRINT(6)	=	number of allowable lines per page of output (default=55)
IPLOT	=	1 for structure plot file, = 0 for no file
MODE(1)	=	-1 for data check
MODE(J)	=	greater than unity for various diagnostics, J=2 to 5, otherwise = 0
MODE(2)	=	-1 for no node number optimization (default is optimization)

MATERIAL PROPERTY DATA

RECORD 4A+: I, MT(I), BSINTG
FORMAT (2I6, E12.0)

where:

I	=	Material property number
	=	-1 to end this data
MT(I)	=	material type 1 = heat conduction 2 = hydrogen diffusion 3 = contact 4 = nonlinear heat conduction 5 = nonlinear contact
BSINTG	=	integration order (default = 2 point Quadrature)

NOTES: If LTYP = 5 in Record 2, two sets of material properties are required, one set of thermal properties and one set of hydrogen diffusion properties. Separate the thermal from hydrogen diffusion properties with a -1. The thermal materials must precede the hydrogen diffusion materials and all materials must be specified consecutively in ascending order.

MATERIAL PROPERTIES

RECORD 4B+: PROP(I,J), J=11
FORMAT (11E12.0)

	MT(I)=1 or 4	MT(I)=2	MT(I)=3 or 5
PROP(I,1) =	mass density	Q, activation energy	contact conductance
PROP(I,2) =	specific heat	Q*, heat of transport	flag for gap sep. *
PROP(1,3) =	conductivity k_x	freq. factor D_x	-
PROP(I,4) =	conductivity k_y	freq. factor D_y	-
PROP(I,5) =	conductivity k_z	freq. factor D_z	-
PROP(I,6) =	heat generation	$C_{dissolution}$	-
PROP(I,7) =	-	$H_{dissolution}$	-
PROP(I,8) =	-	$C_{precipitation}$	-
PROP(I,9) =	-	$H_{precipitation}$	-
PROP(I,10) =	-	solid hydride conc.	-
PROP(I,11) =	-	R, gas constant	-

NOTES: PROP(I,J) are actual material properties when MT(I) = 1, 2, or 3. If MT(I) = 4 or 5, then PROP(I,J) may be scale factors applied to a curve defining temperature dependence of material properties. If MT(I)=3 then

* If PROP(I,2)=0, contact conductance is used as is. If PROP(I,2)≠0, contact conductance is divided by the gap separation. The separation must be finite in order to use this option.

MT(I) = 4, 5, 6,... NONLINEAR MATERIALS

Skip Record 4C+ if MT(I) = 1, 2, or 3

RECORD 4C+ IPROP(I,J), J=1,11
FORMAT(11I6)

IPROP(I,1) = number of curve to be scaled by PROP(I,1)
IPROP(I,2) = number of curve to be scaled by PROP(I,2)
. .
. .
IPROP(I,J) = number of curve to be scaled by PROP(I,J)

NOTES: If IPROP(I,J) = 0, then no curve is used and the scale factor defaults to 1 so that the actual value of PROP(I,J) is used as the material property. If IPROP(I,J) is greater than zero, then a piecewise linear curve is scaled by PROP(I,J) to obtain the temperature dependent material property. If MT(I)=5 then, if IPROP(I,2)=0 average both sides of contact to find T_{avg}
if IPROP(I,2)=1 use 1st side of contact to find T_{avg}
if IPROP(I,2)=-1 use 2nd side of contact to find T_{avg}

CURVE DEFINITION FOR TEMPERATURE DEPENDENT MATERIAL PROPERTIES

Skip RECORDS 5A+ and 5B+ if MT(I) = 1, 2, or 3

RECORD 5A+ TSECT(J,I) (J=1,8)
RECORD 5B+ SECT(J,I) (J=1,8)
FORMAT(8E12.0)

TSECT(J,I) = temperature points in curve definition
SECT(J,I) = function value points in curve definition

NOTES: Records 5A and 5B must come in pairs. There must be exactly as many pairs of records as there are curve numbers used in IPROP(I,J); the maximum value of IPROP(I,J) is assumed to be the number of curves used. Eight or less points may be used to define the curves.

1-D ISOPARAMETRIC CONTINUUM ELEMENT DATA

RECORD 6+: KR, KS, NODI, NODJ, MAT, AREA
FORMAT (5I6,E10.0)

KR	=	number of elements to be generated (default = 1)
	=	-1 to end this data
KS	=	node number difference between adjacent elements (default = 1)
NODI	=	Node number of end I
NODJ	=	Node number of end J
MAT	=	material number, defaults to previous element material number
AREA	=	cross-sectional area (1-D cartesian elements)
	=	thickness (1-D axisymmetric elements)

TWO-DIMENSIONAL ISOPARAMETRIC CONTINUUM ELEMENT DATA

CARD 7+: KR,KS(NODE(J),J = 1,4),MAT,THK
FORMAT (7I6,E10.0)

where:

KR	=	number of elements to be generated (default = 1)
	=	-1 to end this data
KS	=	node number difference between adjacent elements (default = 1)
NODE(J)	=	node numbers defining the plane isoparametric element numbered counter-clockwise (reference Figure 13.9)
MAT	=	material number, defaults to previous material number
THK	=	element thickness, defaults to previous element thickness

NOTES:
(1) For element orientation see Figure 4.1.1.
(2) A triangular element is generated by setting NODE(3) = NODE(4).

THREE-DIMENSIONAL ISOPARAMETRIC CONTINUUM ELEMENT DATA

RECORD 8+: KR,KS(NODE(J),J = 1,8),MAT
FORMAT(11I6)

where:

KR	=	number of elements to be generated (default = 1)
	=	-1 to end this data
KS	=	node number difference between adjacent elements (default = 1)
NODE(J)	=	8 nodes defining the solid isoparametric element
MAT	=	material number defaults to previous material number

NOTES:

(1) Two element types are possible:
   (a) 8 node hexahedron and
   (b) 6 node pentahedron.
   The latter element is specified by setting
   NODE(6) = NODE(7) = NODE(8)

(2) For element orientations, see Figure 4.1.1.

PLATE/SHELL ELEMENT DATA

RECORD 9+: KR, KS, (NODE(J), J = 1,4),MAT, (THK(J),J = 1,4)
FORMAT (7I6,4E10.0)

where:

KR	=	number of elements to be generated (default = 1)
	=	-1 to end this data
KS	=	node number difference between adjacent elements (default = 1)
NODE(J)	=	node number of point J on shell element, numbered counter-clockwise
MAT	=	material number, defaults to previous element material number
THK(J)	=	thickness of shell at node J, defaults to previous element shell thickness. If THK(2), THK(3), THK(4) are zero or not specified, they default to THK(1)

NOTE: (not implemented yet)

1-D CONTACT ELEMENT DATA

RECORD 10: KR, KS, NODI, NODJ, MAT, AREA
FORMAT (5I6,E10.0)

where:

KR	=	number of elements to be generated (default = 1)
	=	-1 to end this data
KS	=	node number difference between adjacent elements (default = 1)
NODI	=	Node number of end I
NODJ	=	Node number of end J
MAT	=	Material number, defaults to previous element material number
AREA	=	Cross-sectional area of contact element

NOTE: Node I and J can have the same coordinates but they must have distinct numbers.

TWO-DIMENSIONAL CONTACT ELEMENT DATA

CARD 11+: KR,KS(NODE(J),J=1,4),MAT,THK
FORMAT (7I6,E10.0)

where:

KR	=	number of elements to be generated (default=1)
	=	-1 to end this data
KS	=	node number difference between adjacent elements (default=1)
NODE(J)	=	node numbers defining the contact element
MAT	=	material number, defaults to previous material number
THK	=	element thickness or width in contact, defaults to previous element thickness

NOTES: (1) For element orientation see Figure 4.2.2.

THREE-DIMENSIONAL CONTACT ELEMENT DATA

RECORD 12+: KR,KS(NODE(J),J=1,8),MAT
FORMAT(11I6)

where:

KR	=	number of elements to be generated (default=1)
	=	-1 to end this data
KS	=	node number difference between adjacent elements (default=1)
NODE(J)	=	8 nodes defining the solid isoparametric element
MAT	=	material number defaults to previous material number

NOTES: (1) For element orientations, see Figure 4.2.2.

CO-ORDINATE DATA

RECORD 13+: J, X(J), Y(J), Z(J), T(J), KN,
(NP Records) FORMAT (I6,4E12.0, I6)

where:

J	=	Node number
	=	-1 to end this data
X(J)	=	X co-ordinate of node J
Y(J)	=	Y co-ordinate of node J
Z(J)	=	Z co-ordinate of node J
T(J)	=	Auxilary nodal data
KN	=	Node number increment for node generation (see Note 1)
	=	0 for no generation

NOTES:

(1) Node data must be specified for NP nodes. They need not be in order but all NP nodes must be defined. Node data for a series of nodes can be generated from the information on two sequential coordinate data records. KN is the node generation parameter given on the first record in the sequence. The generated nodes proceed as J_1 + KN, J_1+KN*2, J_1+KN*3 until J_2-KN is obtained. The node difference of J_2-J_1 must be evenly divisible by KN. Coordinates of generated nodes are linearly interpolated with the remaining data unchanged.

(2) The boundary condition code overrides the master d.o.f. code given on record 1. One active system equation is generated for each unconstrained d.o.f.

IMPOSED NODAL VALUE BOUNDARY CONDITION DATA

If LTFIX=0 skip Record 14.

RECORD 14+: KR,KS,NB,IHIS,BFIX(1)
FORMAT (4I6,E12.0)

where:

KR	=	Number of nodes to be generated (default=1)
	=	-1 to end this data
KS	=	Node number difference between adjacent elements, (default=1)
NB	=	Node number at which temperature or concentration is specified
IHIS	=	number of transient time history curve defining time variation of applied nodal values. (defaults to previous value), (IHIS=0 for steady state analysis, or for constant specified nodal value)
BFIX(1)	=	Value of specified temperature or concentration scale factor at node NB. Used as actual nodal value for steady state analysis or for constant nodal value

If LTFIXH=0 skip Record 14A

RECORD 14A: Repeat Record 14 data for hydrogen diffusion boundary conditions (LTYP=5 only)

APPLIED CONCENTRATED FLUX DATA

If LCONC=0 skip Record 15.

RECORD 15+: KR,KS,NB,IHIS,FORCE(1)
FORMAT (4I6,E12.0)

where:

KR	=	number of nodes to be generated (default=1)
	=	-1 to end this data
KS	=	node number difference between adjacent elements, (default=1)
NB	=	Node number
IHIS	=	number of transient time history curve or for constant flux defining variation of concentrated flux. For steady state analysis, set IHIS=0.
FORCE(1)	=	Concentrated nodal flux scale factor. Used as actual nodal flux value in steady state cases or for constant flux

If LCONCH=0 skip Record 15A

RECORD 15A: Repeat Record 15 for hydrogen diffusion boundary conditions (LTYP=5 only)

APPLIED DISTRIBUTED FLUX DATA

If LPRES = 0, skip Record 16.

RECORD 16: KR,KS,(NODE (I), I=1,4),IHIS,Q
(LPRES Records) FORMAT(7I6,E10.0)

where:

KR	=	number of elements to be generated (default=1)
	=	-1 to end this data
KS	=	node number difference between adjacent elements, (default=1)
NODE(I)	=	Node numbers defining surface subjected to flux "Q". When surface is triangular NODE (4) = 0.
IHIS	=	number of transient time history curve defining time variation of applied distributed flux. (defaults to previous value) (For steady state analysis or for constant flux, set IHIS=0).
Q	=	applied uniform distributed flux scale factor defaults to previous value. Use as actual value of distributed flux in steady state analysis or for constant flux.

Notes: If NODE(3)=NODE(4)=0, the distributed flux is applied either along the edge of a 2-D element or along the length of a 1-D element. In these cases, Q represents a linear flux density. If however, a surface is defined by four distinct nodes, Q represents area flux density.

If LPRESH=0 skip Record 16A

RECORD 16A: Repeat Record 16 for hydrogen diffusion boundary conditions (LTYP=5 only).

THE FOLLOWING DATA IS REQUIRED FOR LINEAR OR NONLINEAR TRANSIENT ANALYSIS (LTYP=2,3,4,5). OTHERWISE SKIP THIS SECTION

RECORD 17: TEND,DELT,DELTA,INTV,NODBLS,KELMBLS,HINTV,HUPINT,TIME
FORMAT (3E10.0,3I6,3E10.0)

where:

TEND	=	time span of response history
DELT	=	time step
DELTA	=	implicit time integration parameter ($0 < DELTA \leq 1$)
INTV	=	interval at which responses to be printed out
NODBLS	=	number of node blocks for which response time history is to be stored on file (≤ 8)
KELMBLS	=	number of element blocks for which element load time history is to be stored on file (≤ 8)
HINTV	=	time interval for time history data (defaults to every time step)
HUPINT	=	time interval to update nonlinear material properties
TIME	=	initial time

If NODBLS = 0 skip RECORD 18

RECORD 18: (NODBL (I,J), J=1,2), I = 1, NODBLS
FORMAT (16I6)

where:

NODBL(I,J)	=	Node number range for which time history of displacement, velocity and acceleration response required to be stored on file ($I \leq 8$) (i.e., NODBL (I,1) = first node number in Block 1, NODBL (I,2) = last node number in Block 1)

If KELMBLS = 0 skip RECORD 19

RECORD 19: (KELMBL (I,J), J=1,2), I = 1, KELMBLS
FORMAT (16I6)

where:

KELM(J)	=	Element number range for which time history of response required to be stored on file ($I \leq 8$)

NOTE: (1) A total of up to 100 nodes and elements is allowed.

RECORD 20+: TIMP(J)
FORMAT (E10.0)

where:

TIMP(J)	=	time at which complete structure response is required
TIMP(J)	=	-1. to end this data (up to 50 times may be specified)

INITIAL CONDITIONS

RECORD 21+: NB, KN, (DISP1(1)
FORMAT (2I6,E12.0)

where:

NB	=	node number
	=	-1 to end this data
KN	=	node number increment for generation (linear interpolation of initial displacements)
	=	0 for no generation
DISP1(1)	=	initial nodal value at node NB

FORCING FUNCTION DEFINITION

RECORD 22: NDT, NHIS, OMEG
FORMAT (2I5,E12.0)

where:

NDT	=	number of time points defining input time history of forcing function (common for all time histories)
NHIS	=	number of time histories ≤ 20
OMEG	=	value of forcing frequency for harmonic forcing function
	=	0.0 for transient forcing function

If NDT = 0, skip RECORD 23+

RECORD 23+: TTIME(J), FORCT(J,I)
FORMAT (2E12.0)
(NHIS*NDT RECORDs)

where:

TTIME(J)	=	Time at point 'J' defining time history
FORCT(J,I)	=	Amplitude of forcing function 'I' at time 'J'

NOTE: (1) If ISUPP = 1, FORCT = Amplitude of acceleration at supports
(2) NHIS sets of records 23+ are required. A common time base must be specified for each time history.

BLISTER GROWTH DATA

RECORD 24+: NBLIS,NBP,DPMAX,DPINC,BLEXP
FORMAT(2I6,3E12.0)

NBLIS	=	number of blisters
NBP	=	number of nodes through thickness at blister
DPMAX	=	maximum blister depth allowable
DPINC	=	increment in blister depth at which to update thermal contact conditions
BLEXP	=	blister expansion factor

RECORD 25+: ((NDBL(I,J),J=1,NBP),I=1,NBLIS)
FORMAT(16I6)

NDBL(I,J)	=	nodes numbers defining a row of nodes through the centre of each blister

THERMAL CYCLE HISTORY DATA

RECORD 26+: NSHUT,SHTEMP
FORMAT (I6,E12.0)

NSHUT	=	number of shutdowns
SHTEMP	=	shutdown temperature of coolant (default value)

RECORD 27+: TSHUT(I),PHT(I)
FORMAT (2E12.0)

TSHUT(I)	=	time of shutdown I
PHT(I)	=	coolant temperature of shutdown I (defaults to SHTEMP)

APPENDIX B

3-D CONTINUUM ELEMENT HOURGLASS CONTROL WITH CONSISTENT MODE CORRECTION FACTORS

Finite element stiffness properties, that are important when modelling nonlinear response, depend on particular details of the element formulation. One method, using one point quadrature to evaluate the stiffness, results in a rank deficient matrix that is corrected by adding the contribution of the independent zero energy (hourglass) modes. The extent of the correction associated with these modes depends on arbitrarily chosen scale factors.

For two dimensional elements, Liu and Belytschko [7] present a means of selecting the scale factor for the single hourglass mode. For rectangular elements, this method yields exact results for full quadrature, the five point finite difference molecule, and the nine point finite difference molecule by choosing different values of the scale factor. A counterpart of this theory for three dimensional elements has not been found in the literature. This appendix presents the derivation of a general theory connecting underintegrated stiffness with hourglass control to the finite element and finite difference theories. The new theory provides an element formulation with features that are important in modelling strong nonlinearities.

B1.1 Background for 2-D Theory

One point quadrature with hourglass correction has been thoroughly examined for two dimensional quad elements. Still, some insight can be gained by revisiting the two dimensional theory with a different approach that will extend more easily to three dimensions. Consider the continuum element in figure B1a for the diffusion equation. The results derived in [7], presented here for comparison purposes, are:

$$B = \frac{1}{A}\begin{bmatrix} b_1^T & b_2^T \end{bmatrix} \qquad b_1 = \frac{1}{2}\begin{bmatrix} y_{24} \\ y_{31} \\ y_{42} \\ y_{13} \end{bmatrix} \qquad b_2 = \frac{1}{2}\begin{bmatrix} x_{42} \\ x_{13} \\ x_{24} \\ x_{31} \end{bmatrix}$$

$$A = \frac{1}{2}\left(x_{31}y_{42} + x_{24}y_{31}\right) \qquad x_{ij} = x_i - x_j \qquad y_{ij} = y_i - y_j \tag{B1}$$

$$x = \begin{bmatrix} x_1 \\ x_2 \\ x_3 \\ x_4 \end{bmatrix} \qquad y = \begin{bmatrix} y_1 \\ y_2 \\ y_3 \\ y_4 \end{bmatrix} \qquad h = \begin{bmatrix} 1 \\ -1 \\ 1 \\ -1 \end{bmatrix}$$

where the x_i and y_i are the coordinates defining the element. The one point quadrature stiffness corrected for the hourglass mode is

$$K = \frac{1}{A}\left(BkB^T\right) + \varepsilon\gamma\gamma^T$$

$$\gamma = h - (h^T x)b_1 - (h^T y)\,b_2 \qquad \text{(B2)}$$

$$\varepsilon = \frac{trace\left(BkB^T\right)}{12A}\,\alpha$$

where the ***trace*** is the sum of the diagonal of a square matrix.

The element stiffness matrix can be viewed as an assemblage of one dimensional elements (links) as per figure B1b, each with a stiffness of the form

$$K_{link} = -k_{ij}\begin{bmatrix} 1 & -1 \\ -1 & 1 \end{bmatrix} \qquad i \neq j \qquad \text{(B3)}$$

Assembled, these links elements provide the element stiffness

$$K^e = \begin{bmatrix} K_1+K_2+K_3 & -K_1 & -K_2 & -K_3 \\ -K_1 & K_1+K_4+K_4 & -K_4 & -K_5 \\ -K_2 & -K_3 & K_2+K_4+K_6 & -K_6 \\ -K_3 & -K_5 & -K_6 & K_3+K_5+K_6 \end{bmatrix} \qquad \text{(B4)}$$

It should be noted that for some element shapes, particularly elements with high aspect ratios, some of the links physically represent conduction through a rod of negative conductivity. However, the assembly of links for the entire element results in a net positive conductivity. For a rectangle, there are generally three different links which are shown in pairs (link sets) in figure B2. If the element is irregular, each link set is represented by the arithmetic average of the links in set, ie.

$$K_1 = \frac{k_{13}+k_{24}}{2} \qquad K_2 = \frac{k_{12}+k_{34}}{2} \qquad K_3 = \frac{k_{23}+k_{14}}{2} \qquad \text{(B5)}$$

With this notation in place, the equation defining ε can be rewritten as

$$\varepsilon = \frac{K_1}{3}\,\alpha \qquad \text{(B6)}$$

This is exactly the same result as given in [7] but a more insightful interpretation is now available. The rectangular element in figure B3 shows the position of integration sampling points defined by the parameter α. Evaluation of the element stiffness by Gauss quadrature using these sampling points results in the link stiffnesses

$$K_1 = -\frac{k(3-\alpha)ab}{12}\left(\frac{1}{a^2} + \frac{1}{b^2}\right)$$

$$K_2 = -\frac{kab}{12}\left(\frac{3+\alpha}{a^2} - \frac{3-\alpha}{b^2}\right) \qquad \text{(B7)}$$

$$K_3 = -\frac{kab}{12}\left(-\frac{3-\alpha}{a^2} + \frac{3+\alpha}{b^2}\right)$$

From these expressions follows the relationship between links

$$(3 - \alpha)(K_2 + K_3) = 2\alpha K_1 \qquad \text{(B8)}$$

which is independent of the element dimensions. When $\alpha = 0$, the dominant conduction path is through the diagonal links and the edge links, K_2 and K_3, average to zero. As α increases, the conductance of the diagonal links shifts to the edge links and finally, when $\alpha = 3$ the diagonal links are zero. With $\alpha = 3$, the links most closely represent physical conducting paths since physically unrealizable negative conductivities are minimized. The significance of this when modelling strong nonlinearities is examined in more detail below.

Upon comparison of the element stiffness (equation B8) obtained from the generalized quadrature and from single point integration with hourglass control leads to the result that both methods are the same for the same value of α. In other words, one point integration with hourglass control corresponds exactly with the generalized four point quadrature for rectangular elements. For nonrectangular elements, the same interpretation applies except that the correspondence is no longer exact. The degree of approximation depends on how different the element is from a perfect rectangle. The relationship between the hourglass control and other methods is now readily apparent. For $\alpha = 1$ the sampling points coincide with 2 point Gauss-Legendre quadrature and the standard finite element method is obtained. The trapezoidal integration is obtained with $\alpha = 3$, and as discussed in [7] this result corresponds to the finite difference five point molecule.

B1.2 Preliminaries for 3-D Theory

Before proceeding with the derivation of the three dimensional hourglass control theory for isotropic diffusion, some terminology is required. A box element (defined as a rectangular parallelepiped) can be regarded as an assemblage of 28 two noded elements connecting each pair of nodes defining the box element. This is exactly the same situation as for the 2-D case except more links are required to define one 3-D element. The 28 links in the box element can be grouped into seven sets of four equal links as shown in figure B4. The links in a given set have equal stiffnesses so just one stiffness value per set is required. The scalar K_n, n = 1 to 7, is defined as the stiffness for link set n such that $K_n = k_{ij}$ when i and j are both nodes of a link in link set n.

The links in a link set are defined only in terms of node numbers so that link sets can be identified for arbitrary hex elements. Note that the order of the link set definition as it relates to the node numbering convention of the element is important. For irregular hexahedrons, the links in a link set are not generally equal so K_n is defined as the arithmetic average of the four links in set n.

When the element stiffness is evaluated using the generalized Gauss quadrature, the link stiffnesses are

$$K_n = \frac{9kL_1L_2L_3(3-\alpha)}{16}\left[\frac{6}{L_n^2} - (3+\alpha)\left(\frac{1}{L_1^2}+\frac{1}{L_2^2}+\frac{1}{L_3^2}\right)\right] \qquad n = 1,2,3$$

$$K_4 = -\frac{9kL_1L_2L_3(3-\alpha)^2}{16}\left(\frac{1}{L_1^2}+\frac{1}{L_2^2}+\frac{1}{L_3^2}\right) \tag{B9}$$

$$K_{n+4} = \frac{9kL_1L_2L_3(3+\alpha)}{16}\left[(3-\alpha)\left(\frac{1}{L_1^2}+\frac{1}{L_2^2}+\frac{1}{L_3^2}\right) - \frac{6}{L_n^2}\right] \qquad n = 1,2,3$$

where the L_n are the element dimensions as indicated in figure B4. Only three of these equations are independent since for arbitrary dimensions of the element the following relations hold:

$$K_n + \left(\frac{3-\alpha}{3+\alpha}\right)K_{n+4} = \left(\frac{2\alpha}{3-\alpha}\right)K_4 \qquad n = 1,2,3$$

$$(3-\alpha)(K_1+K_2+K_3) = 3(1+\alpha)K_4 \tag{B10}$$

The first three of equations (B9) along with equations (B10) completely define all stiffness properties for box elements.

B1.3 3-D Hourglass Control

In view of the results given above for the two dimensional case, the relationship between the one point quadrature with hourglass control and the generalized quadrature method is hypothesized to exist for the three dimensional case. Before testing this hypothesis, the hourglass control theory is presented briefly.

The hourglass correction is obtained from

$$K = K^{1x1} + K^h$$
$$K^h = \sum e_n \gamma_n \gamma_n^T \tag{B11}$$

The gamma vectors are determined from

$$\gamma_n = h_n - \left(h_n^T x\right)b_1 - \left(h_n^T y\right)b_2 - \left(h_n^T z\right)b_3 \tag{B12}$$

where

$$h_1 = \begin{bmatrix} 1 \\ -1 \\ 1 \\ -1 \\ 1 \\ -1 \\ 1 \\ -1 \end{bmatrix} \quad h_2 = \begin{bmatrix} 1 \\ 1 \\ -1 \\ -1 \\ -1 \\ -1 \\ 1 \\ 1 \end{bmatrix} \quad h_3 = \begin{bmatrix} 1 \\ -1 \\ -1 \\ 1 \\ -1 \\ 1 \\ 1 \\ -1 \end{bmatrix} \quad h_4 = \begin{bmatrix} 1 \\ -1 \\ 1 \\ -1 \\ -1 \\ 1 \\ -1 \\ 1 \end{bmatrix} \tag{B13}$$

represent the four hourglass mode vectors physically depicted in figure B5, and $\mathbf{b}_1$, $\mathbf{b}_2$, and $\mathbf{b}_3$ are arrays of the derivatives of the shape functions with respect to x, y, and z respectively evaluated at the centroid of the element. Four nonzero values of ε_n in equation B11 can be arbitrarily specified to ensure that K is not rank deficient. Here, the ε_n are to be chosen so that the hourglass correction defines the same result obtained by the generalized quadrature. It is presupposed that there exist four distinct ε_n that are functions of α and the one point integration stiffness results. Equations (B10) are four independent conditions that can be used to determine the ε_n. The K_n in equations (B10) are written in terms of K^{1x1} and the ε_n by using equation (B11). This procedure provides four linear equations that are routinely solved and rearranged to

$$\begin{pmatrix} \varepsilon_1 \\ \varepsilon_2 \\ \varepsilon_3 \\ \varepsilon_4 \end{pmatrix} = \begin{bmatrix} -\frac{\alpha}{6}\begin{bmatrix} 1 & 0 & 0 & 1 \\ 0 & 1 & 0 & 1 \\ 0 & 0 & 1 & 1 \end{bmatrix} \\ \frac{-\alpha^2}{9}\begin{bmatrix} 0 & 0 & 0 & 1 \end{bmatrix} \end{bmatrix} \begin{pmatrix} K_1 \\ K_2 \\ K_3 \\ K_4 \end{pmatrix} \tag{B14}$$

If desired, equation (B10) can be used to eliminate K_4 from equation (B14) thus defining the epsilons in terms of the three independent face diagonal links,

$$\begin{pmatrix} \varepsilon_1 \\ \varepsilon_2 \\ \varepsilon_3 \end{pmatrix} = -\frac{\alpha}{6}\begin{bmatrix} 2 & 1 & 1 \\ 1 & 2 & 1 \\ 1 & 1 & 2 \end{bmatrix} \begin{pmatrix} K_1 \\ K_2 \\ K_3 \end{pmatrix} \tag{B15}$$

$$\varepsilon_4 = \frac{\alpha}{6}(\varepsilon_1 + \varepsilon_2 + \varepsilon_3)$$

The symmetry of equation (B15) is an interesting result since it clearly shows that each hourglass mode has its own scale factor. Unless the element is a square prism or a cube, each scale factor is unique. The form of equation (B15) indicates that the first three hourglass modes are similar in nature, and by referring to figure B5, it is seen that element edges corresponding to K_{n+4} and K_n are not stretched by mode n, n = 1,2,3. The fourth mode is special since it stretches all edges of

the element. The specification of ε_n is such that for the first three modes, the larger K_n is, the larger the scale factor for mode n will be regardless of the choice of α. The fourth mode scale factor has a quadratic dependence on α so for small α, this correction term is smaller than the other factors, but as α increases, ε_4 eventually exceeds the other scale factors.

Perhaps the most important aspect of this development is that arbitrarily choosing ε_n is not appropriate even for "small" values. This is supported by the fact that for small α (say .05) the fourth mode scale factor should be considerably less than the other modes. Also, for elements with large aspect ratios, the scale factor for mode corresponding to shortest edges of the element must be higher than the other scale factors. Basing all four scale factors on a single arbitrary parameter results in a consistent procedure for applying hourglass control regardless of the proportions of the element. Hence, the correction factors are called consistent mode correction factors.

B1.4 3-D Theory for Arbitrary Element Shapes

The consistent mode correction method clearly makes an important connection between standard finite element methods and underintegrated stiffness with hourglass control. However, the above theory is developed only for the special case of box elements. This is of limited use since in general, finite element methods depend on the ability to discretize irregular domains with elements of arbitrary shape.

It is stated above that the 2-D theory is applicable to nonrectangular elements when average values for link stiffness are used, and this same approach can be used for 3-D elements. With

$$K_1 = \frac{k_{13} + k_{24} + k_{57} + k_{68}}{4} \qquad K_2 = \frac{k_{18} + k_{45} + k_{27} + k_{36}}{4} \qquad K_3 = \frac{k_{16} + k_{25} + k_{38} + k_{47}}{4}$$

$$K_4 = \frac{k_{17} + k_{28} + k_{35} + k_{46}}{4} \qquad \text{(B16)}$$

$$K_5 = \frac{k_{15} + k_{26} + k_{37} + k_{48}}{4} \qquad k_6 = \frac{k_{12} + k_{34} + k_{56} + k_{78}}{4} \qquad K_7 = \frac{k_{14} + k_{23} + k_{58} + k_{67}}{4}$$

equations (B10) still hold but only for the average of links in a link set rather than for individual links. The connection with a 2x2x2 quadrature finite element derivation is now only approximate in the sense that the determinant of the Jacobian is assumed to be constant over the element with a value equal to that at the centroid. In general, the Jacobian is a variable except for the special case of parallelpiped elements. An additional approximation occurs because material properties are also assumed to be constant (centroidal values) spatially within the element. Just how much error is involved in ignoring the variation of the Jacobian is roughly dependent on how skewed the element is. The effect of ignoring variation of material properties depends on the strength of material nonlinearities as well as on the magnitude of gradients of nodal variables across the element.

The hourglass control scale factors obtained from a general element can be viewed as if they were determined from a box element of similar length, width and height to the general element as indicated in figure B6 for quadrilaterals. In this way, the consistent hourglass control method

approximately takes into account the aspect ratios of elements of arbitrary shape when determining the hourglass control stiffness. Other published works use one and the same scale factor for all of the hourglass modes.

The connection between the consistent mode hourglass control and the finite difference method for 3-D elements is indeed met for box elements with alpha = 3. In this case, the element stiffness has only edge links with nonzero values and all four diagonal link sets are zero. It should be noted that regardless of aspect ratios, these edge link stiffnesses individually represent conduction paths with positive conductivity. For arbitrary 3-D elements, this is not the case. Since the links in a diagonal link set average to zero, unless each link is exactly zero (only for box elements), some of the links must necessarily represent negative conductivity. However, the magnitude of negative conductivity links is minimized by this method. In practice, increasing alpha has the net effect of increasing the emphasis of positive conductivity in the edge links while at the same time reducing the conductivity of the diagonal links. This property is significant in the special treatment of strong nonlinearities by adjusting individual link stiffnesses according to material property variation.

Incorporation of the consistent mode method into a 3-D finite element program requires only a small effort due simplifications resulting from the special form of the underintegrated stiffness matrix. From equation B15, only K_1, K_2, and K_3 are required to determine epsilon. For isotropic materials,

$$K_1 = \frac{k_{13} + k_{24}}{2}, \qquad K_2 = -\frac{k_{12} + k_{34}}{2}, \qquad K_3 = -\frac{k_{14} + k_{23}}{2} \tag{B17}$$

so that only six components of $K^{[a]}$ need to be evaluated explicitly to compute epsilon. If the actual stiffness matrix is required, these six stiffness components in equation B17 are needed anyway, and the actual cost of determining epsilon is negligible. In a typical explicit algorithm utilizing one point quadrature, stiffness components are not usually determined directly so there is some extra computational cost involved in computing epsilon. However, when programming numerical methods, efficiency should yield to correctness. The additional computations can be avoided by storing the values for epsilon (only three independent values per element) although this increases memory requirements slightly.

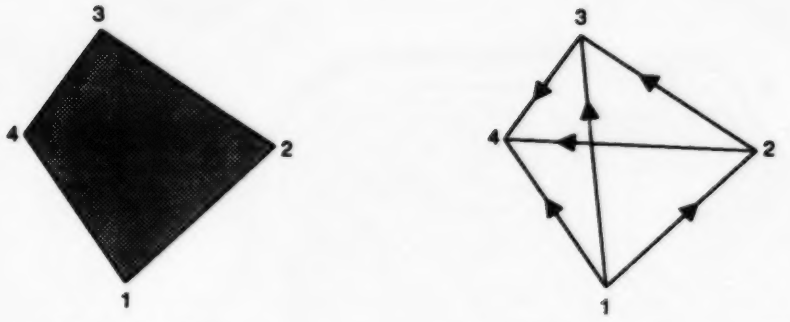

(a) Continuum Element

(b) Element Represented by Network of Conducting Links

FIGURE B1

LINK REPRESENTATION OF CONTINUUM ELEMENT

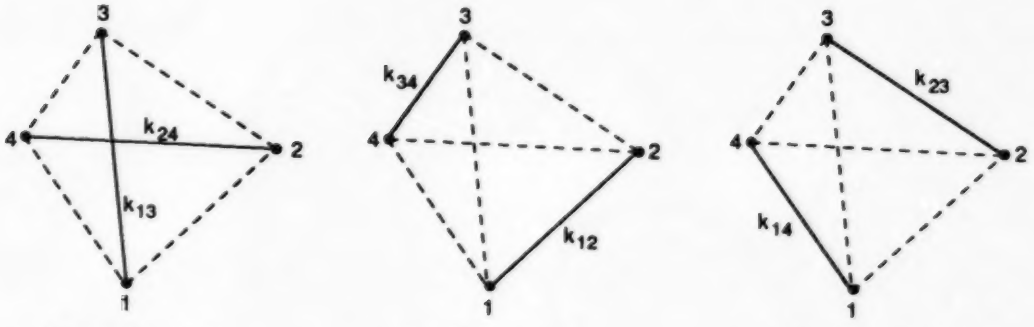

$K_1 = 1/2\,(k_{13} + k_{24})$ (a) Set 1

$K_2 = 1/2\,(k_{12} + k_{34})$ (b) Set 2

$K_3 = 1/2\,(k_{14} + k_{23})$ (c) Set 3

FIGURE B2

LINK SETS FOR 2-D ELEMENT

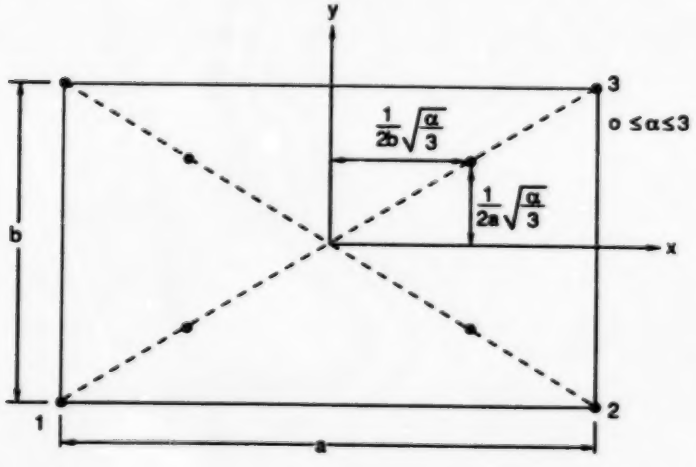

FIGURE B3

SAMPLING POINTS FOR GENERALIZED GAUSS QUADRATURE

91-102-K

185646-S63-RD

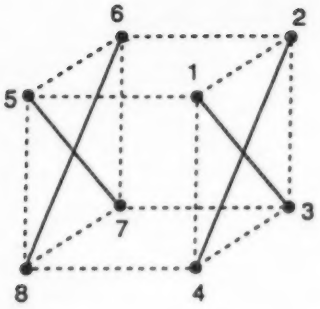

Set 1

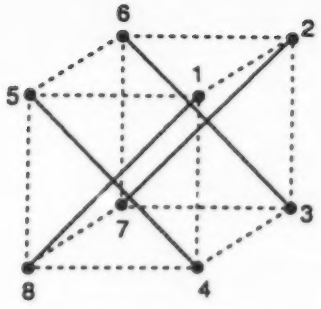

Set 2

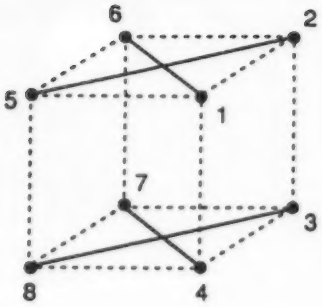

Set 3

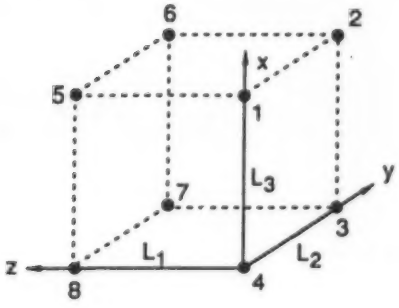

Dimensions

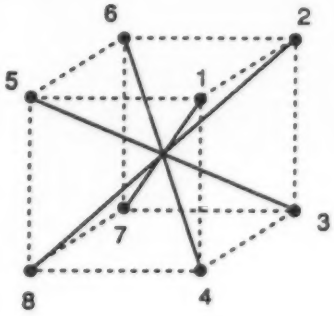

Set 4

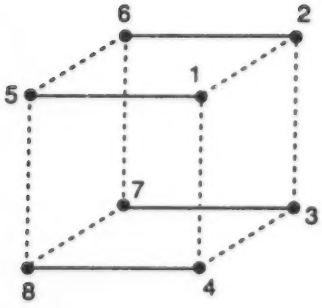

Set 5

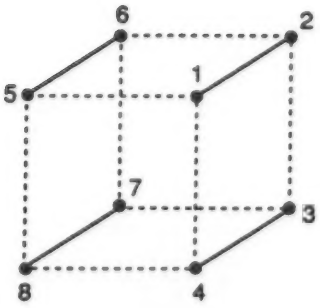

Set 6

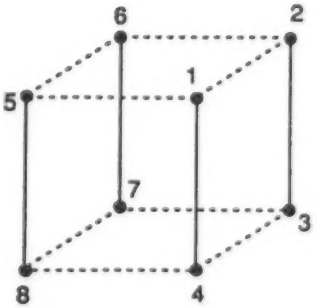

Set 7

FIGURE B4

LINK SETS FOR 3-D CONTINUUM ELEMENT

91-102-K

185650-S63-RD

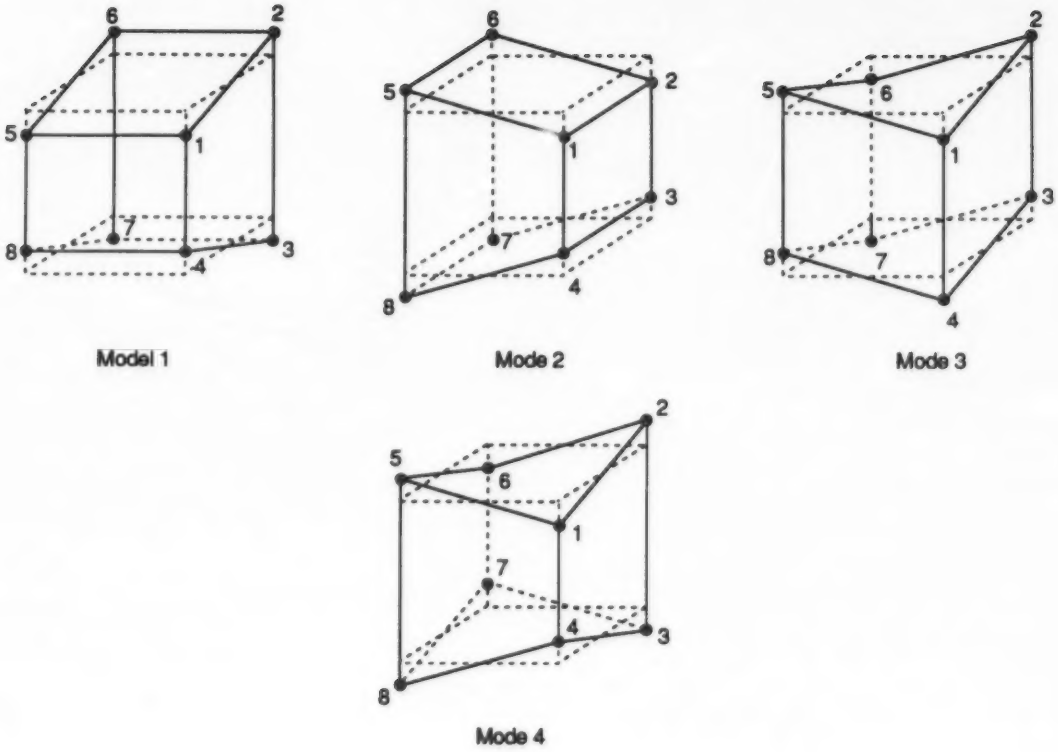

FIGURE B5

HOURGLASS MODES SHOWN AS DEFORMATION MODES OF A CUBE

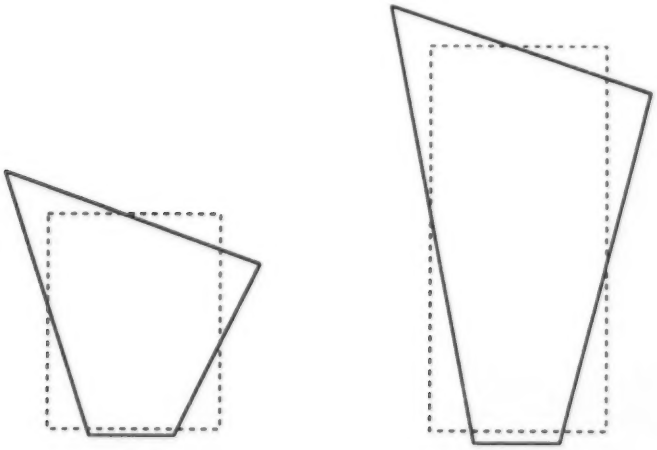

FIGURE B6

ASPECT RATIOS OF IRREGULAR QUADRILATERALS

91-102-K
185651-S63-RD